Stress Evaluation During Bathing by Analysis of Bathtub Electrocardiogram

LI Tianhui

A DISSERTATION

SUBMITTED IN FULFILLMENT OF THE REQUIREMENTS

FOR THE DEGREE OF DOCTOR OF PHILOSOPHY

IN COMPUTER SCIENCE AND ENGINEERING

Graduate Department of Computer and Information Systems
The University of Aizu
2022

The thesis titled

Stress Evaluation during Bathing by Analysis of Bathtub Electrocardiogram

By

LI Tianhui

is reviewed and approved by:

Chief referee *Professor* *CHEN Wenxi*	Wenxi Chen	2022/8/17
Professor *COHEN Michael*	Michael Cohen	2022/8/30
Associate Professor *HISADA Yasuhiro*	Hisada Yasuhiro	2022/8/18
Associate Professor *YEN Neil Yuwen*	Neil Yen	2022/8/17

THE UNIVERSITY OF AIZU

2022

Contents

List of Figures

List of Tables

List of Abbreviations

ANS	Autonomic Nervous System
BLE	Bluetooth Low Energy
BP	Blood Pressure
BT	Bathing Test
BTp	Body Temperature
BW	Body Weight
CAD	Coronary Artery Disease
DBP	Diastolic Blood Pressure
DFA	Detrended Fluctuation Analysis
ECG	Electrocardiogram
EEG	Electroencephalogram
EMG	Electromyogram
EST	Exercise Stress Test
HF	High Frequency
HFnu	Normalized High Frequency Power
HR	Heart Rate
HRV	Heart Rate Variability
IBI	Interbeat interval
KNN	K-Nearest Neighbor
kSQI	Kurtosis
NL	Noise Limit
NNI	Normal R-peak to Normal R-peak Interval

PC	Principal Component
PCA	Principal Component Analysis
pcaSQI	Principal Component Analysis SQI
PNS	Parasympathetic Nervous System
pSQI	Relative Power in the QRS Complex
RMSSD	Root Mean Square of Successive NNI Differences
RRI	R-peak to R-peak Interval
rSQI	Undetected Error of R-peaks
R1	Resting Stage
R2	Recovery Stage
R3	Relax Stage
R^2	Coefficient of Determination
SampEn	Sample Entropy
SBP	Systolic Blood Pressure
SI	Stress Index
SNS	Sympathetic Nervous System
SQI	Signal Quality Index
SSE	Sum of Squares Due to Error
TP	Algorithm of Pan & Tompkins
USB	Universal Serial Bus
2-D	Two-Dimensional
℃	Celsius Degrees

List of Symbols

x	Heart Rate Variability feature
Z	Normalized value of the HRV feature
E	Expectation
μ	Mean
δ	Standard deviation
D	Euclidean distance
X_{BT}	Abscissa value of the BT feature point
X_{EST}	Abscissa value of the EST site point
Y_{BT}	Ordinate value of the BT feature point
Y_{EST}	Ordinate value of the EST site point
ST	Equivalent exercise stress test stage
WT	Water temperature of the bathing test
BD	Bathing duration of the bathing test
ST_m	Original values of the equivalent exercise stress test grouped stage
$\widehat{ST}_m$	Fitted values of the equivalent exercise stress test grouped stage
M	Number of sets of samples

Abstract

With the rapid economic development and the accelerating pace of life, people are confronted with ever-increasing stress from all aspects of the study, work, and living. Stress has gradually become one of the main factors affecting the physical health of individuals. Some biosignals are applied to evaluate the stress including Electrocardiogram (ECG), Electroencephalogram (EEG), and Electromyogram (EMG), et al. In the dissertation, ECG signals are used to evaluate stress.

ECG is the process of recording the heart's electrical activity over time. It is a conventional biosignal of medical diagnosis. There are three main components in an ECG signal: the P wave; the QRS complex; and the T wave. Detected R peaks can be used to calculate the R-peak to R-peak Interval (RRI) to complete heart rate variability (HRV) analysis in time, frequency, and nonlinear domain. Since the early commercial ECG device was applied in 1901, ECG device has improved with the development of technology. However, these devices still have some inconveniences during using. Bathing is a part of the daily routine for most Japanese people. In addition to daily cleaning, bathing can also be used as a means of daily healthcare monitoring. In the dissertation, a bathtub ECG monitoring system is used to collect ECG signals during bathing.

In this dissertation, the bathtub ECG monitoring system is optimized. The most suitable electrode for bathtub ECG collection during bathing is selected based on the evaluation of the ECG signal quality. Using HRV analysis to estimate the optimal bathing time, combined with the stress index, the effect of stress on the optimal bathing time is obtained. Stress has an obvious effect on optimal bathing time. Stress increases the optimal bathing time. In high-stress situations, it takes longer to achieve the comfort of bathing. Bathtub ECG as a potential alternative to light stress test in daily life is proposed. The correlation between bathing and exercise stress test (EST) is explored. The relationship between bathing duration, water temperature, and the EST stage is analyzed. Twenty-three HRV features are used to group different bathing conditions corresponding to the EST stages using the Voronoi diagram method in terms of HRV behaviors. In all equivalent EST stages of bathing tests at the five water temperatures, the low stage, medium stage, and high stage account for 17.86%, 52.86%, and 29.29%, respectively. The higher water temperatures and longer bathing durations in the bathing test correspond to higher stages in the EST. The bathing test at the most severe condition of 41°C and 15 min corresponds to a high EST stage in terms of HRV behavior. Daily bathing can serve not only for cleaning and healthcare monitoring but also as a reference for an at-home alternative to the EST. The organization and main contribution of this dissertation are briefly summarized in the following manner.

Chapter 1 first offers an introduction and background on ECG, HRV, bathtub ECG system, and stress monitoring.

Chapter 2 describes the effect of stress on optimal bathing time. Using HRV analysis to estimate the optimal bathing time, combined with the stress index, the effect of stress on the optimal bathing time is obtained. Stress has an obvious effect on optimal bathing time. Stress delays the optimal bathing time. In high-stress situations, it takes longer to achieve the comfort of bathing.

In order to improve the bathtub ECG monitoring system, Chapter 3 describes the bathtub ECG monitoring system is optimized based on the most suitable electrode. The most suitable electrode for bathtub ECG collection during bathing is selected based on the evaluation of the ECG signal quality including four signal quality indices.

Chapter 4 describes the bathtub ECG as a potential alternative to light stress test in daily life. A bathtub ECG as a potential alternative to light stress test in daily life is proposed. The correlation between bathing and exercise stress test is explored. The relationship between bathing duration, water temperature, and the EST stage is analyzed.

Finally, the present work is summarized, and future research directions are discussed in Chapter 5.

Chapter 1

Introduction

It has been found a significant increase in anxiety, depression, pathological stress, and other stress-related diseases in recent years. Generally, human physical and mental health and well-being can be damaged by stress [1,2,3]. Stress is a feeling of emotional or physical tension, and it can be caused by anything you feel angry, uncomfortable, or nervous about. Stress is your body's reaction when feeling under pressure or threatened. It usually can be not controlled when stress happens. Stress is your body's reaction to a challenge or demand. It is necessary to maintain complex homeostasis in the body. Homeostasis is constantly challenged by stressors including inside or outside adverse forces. Stress arises when homeostasis is threatened [4]. In the short term, stress can be positive, such as you meet a deadline under stress status. But your health can be damaged under continuous stress in the long term. Stress is frequently cited as an important contributor to disease, and more and more clinical evidence has been showing the effects of stress on the immune and cardiovascular systems. In particular, the risks of developing cardiovascular disease, diabetes, stroke, and obesity can be increased by chronic stress [5,6,7,8]. Stress affects health in two means including direct and indirect. Health can be affected directly through the response of the

autonomic nervous system (ANS) caused by stress. Stress also can indirectly affect health through changes in health behaviors [9].

According to the statistics from the World Health Organization, stress is associated with several medical and social problems that disproportionately affect not only adults but also the health and well-being of children and adolescents [10]. Failure to address adolescent mental health has consequences that extend into adulthood, impairing physical and mental health. Consequently, there has been great interest in studying the underlying mechanisms of stress and monitoring the various physiological and biochemical responses of the body to stress [11].

In the past two decades, many excellent studies have confirmed that stress affects the brain [12,13,14] and ANS [9,15,16,17]. With the considerable development of technology, biosignals can be measured reliably to provide accurate monitoring of stress, potentially preventing diseases early.

Contact monitoring has the potential to place an additional burden on the subjects during biosignals monitoring. Therefore, the unconscious, unrestrained, and noncontact acquisition method is more suitable for biosignal monitoring for stress. Bathing is a part of the daily routine for most Japanese people. In addition to the role of daily cleaning, bathing also can be used as a means of daily healthcare monitoring. Biosignals monitoring can be unconsciously, unrestrainedly, and noncontact implemented during bathing. As a conventional biosignal for medical diagnosis, ECG is more convenient to collect during

bathing than other biosignals.

In this dissertation, stress is evaluated during bathing by analysis of bathtub ECG. A bathtub ECG monitoring system is used to collect ECG signals during bathing. The effect of stress on optimal bathing is explored. The relationship among stress, bathtub water temperature, and bathing duration is discussed. The relationship between different stressors such as exercise and bathing is explored.

There are three studies in this dissertation. First study is in Chapter 2. Chapter 2 describes the effect of stress on optimal bathing time. Using HRV analysis to estimate the optimal bathing time, combined with the stress index, the effect of stress on the optimal bathing time is obtained. Stress has an obvious effect on optimal bathing time. Stress delays the optimal bathing time. In high-stress situations, it takes longer to achieve the comfort of bathing.

To improve the bathtub ECG monitoring system, Chapter 3 describes the bathtub ECG monitoring system is optimized based on the most suitable electrode. The most suitable electrode for bathtub ECG collection during bathing is selected based on the evaluation of the ECG signal quality including four signal quality indices.

Chapter 4 describes the bathtub ECG as a potential alternative to light stress test in daily life. A bathtub ECG as a potential alternative to light stress test in daily life is proposed. The correlation between bathing and exercise stress test is explored. The relationship between bathing duration, water temperature, and the

EST stage is analyzed.

1.1 Electrocardiogram

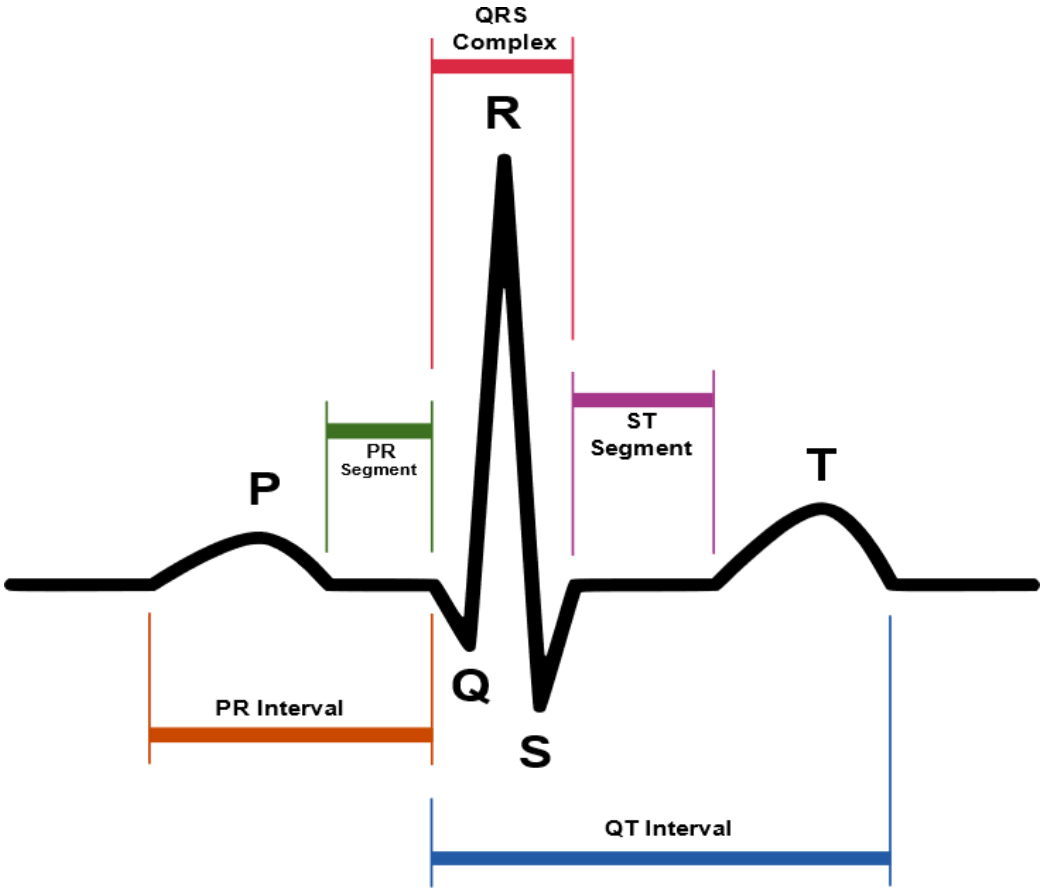

Figure 1: ECG of a heartbeat in normal sinus rhythm

ECG is the process of recording the electrical activity of the heart over a period of time using electrodes placed on the skin. These electrodes detect the

tiny electrical changes on the skin that arise from the heart muscle's electrophysiologic pattern of depolarizing and repolarizing during each heartbeat. It is very commonly performed to detect any cardiac problems [18].

There are three main components in an ECG: the P wave, which represents the depolarization of the atria; the QRS complex, which represents the depolarization of the ventricles; and the T wave, which represents the repolarization of the ventricles, as shown in Figure 1. During each heartbeat, a healthy heart has an orderly progression of depolarization that starts with pacemaker cells in the sinoatrial node, spreads throughout the atrium, passes through the atrioventricular node down into the bundle of His and into the Purkinje fibers, spreading down and to the left throughout the ventricles [19]. This orderly pattern of depolarization gives rise to the characteristic ECG tracing. To the trained clinician, an ECG conveys a large amount of information about the structure of the heart and the function of its electrical conduction system [20]. Among other things, an ECG can be used to measure the rate and rhythm of heartbeats, the size and position of the heart chambers, the presence of any damage to the heart's muscle cells or conduction system, the effects of heart drugs, and the function of implanted pacemakers [21]. ECG signals are used to diagnose various cardiac diseases, including arrhythmia, myocardial infarction, ventricular hypertrophy, coronary artery disease, and ischemic heart disease, et al. [22,23,24,25,26]. ECG also has important clinical value for non-cardiac conditions such as apnoea, pulmonary embolism, and esophageal disorders [27,28].

The 12-lead ECG is one of the most commonly clinical cardiac medicine diagnostic tools. The 12-lead ECG signals are collected using attaching ten electrodes on the surfaces of limbs and the chest as shown in Figure 2. Electrical activities of the heart are recorded from the frontal and the horizontal views to group 12 channels of ECG signals based on the ten electrodes.

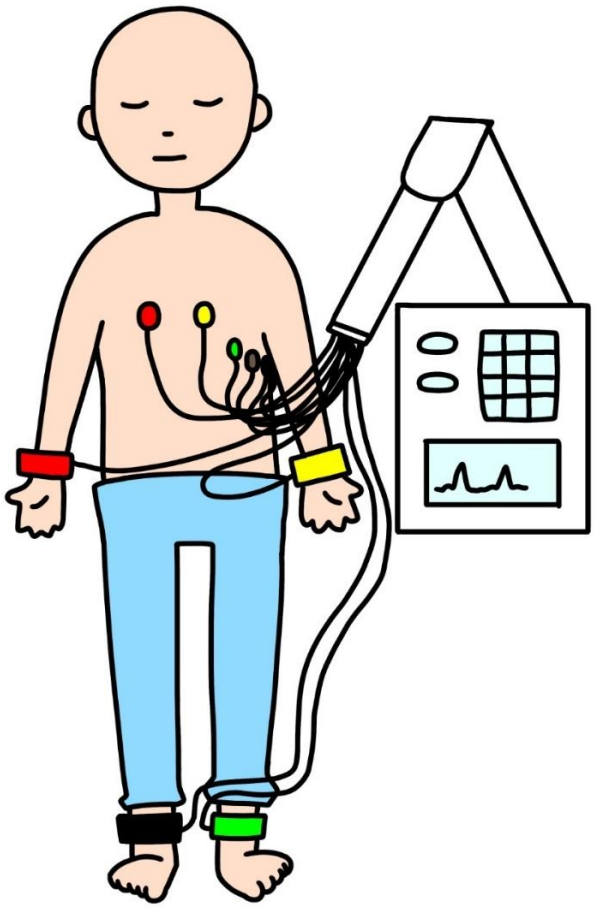

Figure 2: 12-Lead ECG electrode placement

Of the three main components of ECG signal, the R-peak is the most frequently detected for analysis. Detected R-peaks can be used to calculate the R-peaks to R-peaks interval (RRI) as shown in Figure 3. The heart rate variability (HRV) analysis is implement based on the RRI. The HRV features in time-,

frequency-, and nonlinear domain are used to explain the electrical activities of the heart.

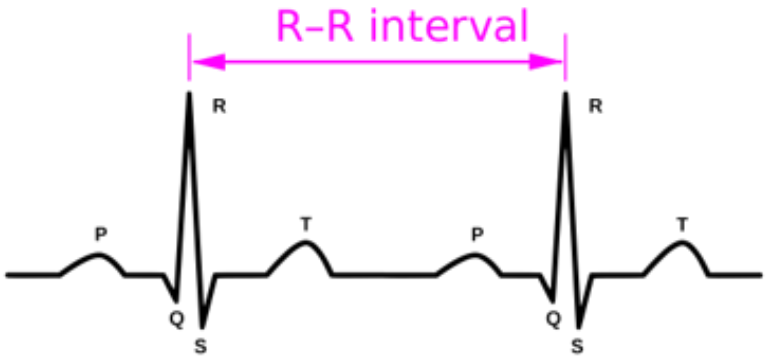

Figure 3: RRI between two heartbeats in normal sinus rhythm

1.2 Heart Rate Variability

HRV is the physiological phenomenon of variation in the time interval between heartbeats. It is measured by the variation in the beat-to-beat interval [29]. HRV is thought to reflect the heart's ability to adapt to changing circumstances by detecting and quickly responding to unpredictable stimuli. HRV analysis is the ability to assess overall cardiac health and the state of the ANS responsible for regulating cardiac activity [30]. The normal variability in heart rate (HR) is due to autonomic neural regulation of the heart and the circulatory system [31]. The balancing action of the sympathetic nervous system (SNS) and parasympathetic nervous system (PNS) branches of the ANS controls the HR. Increased SNS or diminished PNS activity results in cardio-acceleration. Conversely, a low SNS activity or a high PNS activity causes cardio-deceleration. The degree of variability in the HR provides information about the functioning of the nervous control on the HR and the heart's ability to respond.

The past few decades have witnessed an important relationship between ANS and cardiovascular mortality [32, 33, 34]. Numerous papers appeared in connection with HRV related cardiological issues reaffirm the importance of HRV in assessing the cardiac health [35, 36, 37, 38, 39, 40, 41, 42]. Kovatchev et al. introduced the sample asymmetry analysis and demonstrated its utility in assessing HR characteristics occurring, early in the course of neonatal sepsis and

systemic inflammatory response syndrome [43]. Tulen et al. found HR, diastolic blood pressure (DBP), mid-frequency band power of HR and systolic blood pressure (SBP), and plasma adrenaline concentrations showed significant increase when changed from supine to sitting to standing posture [44]. Verlinde et al. compared the HRV of aerobic athletes with the controls and showed that the aerobic athletes have an increased power in all frequency bands [45]. With the advent of low cost computers with massive computational power, much progress was achieved in the field which fueled many advances. HRV has become the conventionally accepted term to describe variations of both instantaneous heart rate and RRI.

24 h, short-term (~5 min), and ultra-short-term (<5 min) HRV can be described using time-domain, frequency-domain, and non-linear measurements. HRV features in time-domain quantify the amount of variability in measurements of the interbeat interval (IBI). The IBI is the time between successive heartbeats, generally, it is a normal peak to a normal peak interval (NNI). The HRV time domain measures as illustrated in Table 1 [46].

Table 1. HRV time–domain measures.

Feature	Unit	Description
SDNN	ms	Standard deviation of all NNIs
SDRR	ms	Standard deviation of all RRIs
SDANN	ms	Standard deviation of the average NNIs for each 5 min segment of a 24 h HRV recording
SDNN Index (SDNNI)	ms	Mean of the standard deviations of all the NNIs for each 5 min segment of a 24 h HRV recording
NN50	count	Number of pairs of adjacent NNIs differing by more than 50 ms in the entire recording
pNN50	%	NN50 divided by the total number of all NNIs
RMSSD	ms	The square root of the mean of the sum of the squares of differences between adjacent NNIs
HR Max −HR Min	bpm	Average difference between the highest and lowest heart rates during each respiratory cycle
TINN	ms	Baseline width of the RRI histogram
HRV triangular index		Total number of all NNIs divided by the height of the histogram of all NNIs measured on a discrete scale

Frequency-domain measurements estimate the distribution of absolute or relative power into four frequency bands. The Task Force of the European Society of Cardiology and the North American Society of Pacing and Electrophysiology (1996) divided HR oscillations into four frequency bands, including ultra-low-frequency (ULF), very-low-frequency (VLF), low frequency (LF), and high frequency (HF) bands as illustrated in Table 2 [46].

HRV non-linear measurements can quantify the unpredictability of a time series as illustrated in Table 3 [46].

Table 2. HRV frequency–domain measures.

Feature	Unit	Description
ULF	ms^2	Absolute power of the ultra-low-frequency band (≤0.003 Hz)
VLF	ms^2	Absolute power of the very-low-frequency band (0.0033 – 0.04 Hz)
LF peak	Hz	Peak frequency of the low-frequency band (0.04 – 0.15 Hz)
LF	ms^2	Absolute power of the low-frequency band (0.04 – 0.15 Hz)
LF norm	nu	Relative power of the low-frequency band (0.04 – 0.15 Hz) in normal units
LF power	%	Relative power of the low-frequency band (0.04 – 0.15 Hz)
HF peak	Hz	Peak frequency of the high-frequency band (0.15 – 0.4 Hz)
HF	ms^2	Absolute power of the high-frequency band (0.15 – 0.4 Hz)
HF norm	nu	Relative power of the low-frequency band (0.15 – 0.4 Hz) in normal units
HF power	%	Relative power of the low-frequency band (0.15 – 0.4 Hz)
LF/HF	%	Ratio of LF to HF power

Table 3. HRV nonlinear measures.

Feature	Unit	Description
S	ms	Area of the ellipse which represents total HRV
SD1	ms	Poincaré plot standard deviation perpendicular to the line of identity
SD2	ms	Poincaré plot standard deviation along the line of identity
SD1/SD2	%	Ratio of SD1 to SD2
ApEn		Approximate entropy, which measures the regularity and complexity of a time series
SampEn		Sample entropy, which measures the regularity and complexity of a time series
DFA α1		Detrended fluctuation analysis, which describes short-term fluctuations
DFA α2		Detrended fluctuation analysis, which describes long-term fluctuations
D_2		Correlation dimension, which estimates the minimum number of variables required to construct a model of system dynamics

1.3 Bathtub Electrocardiogram System

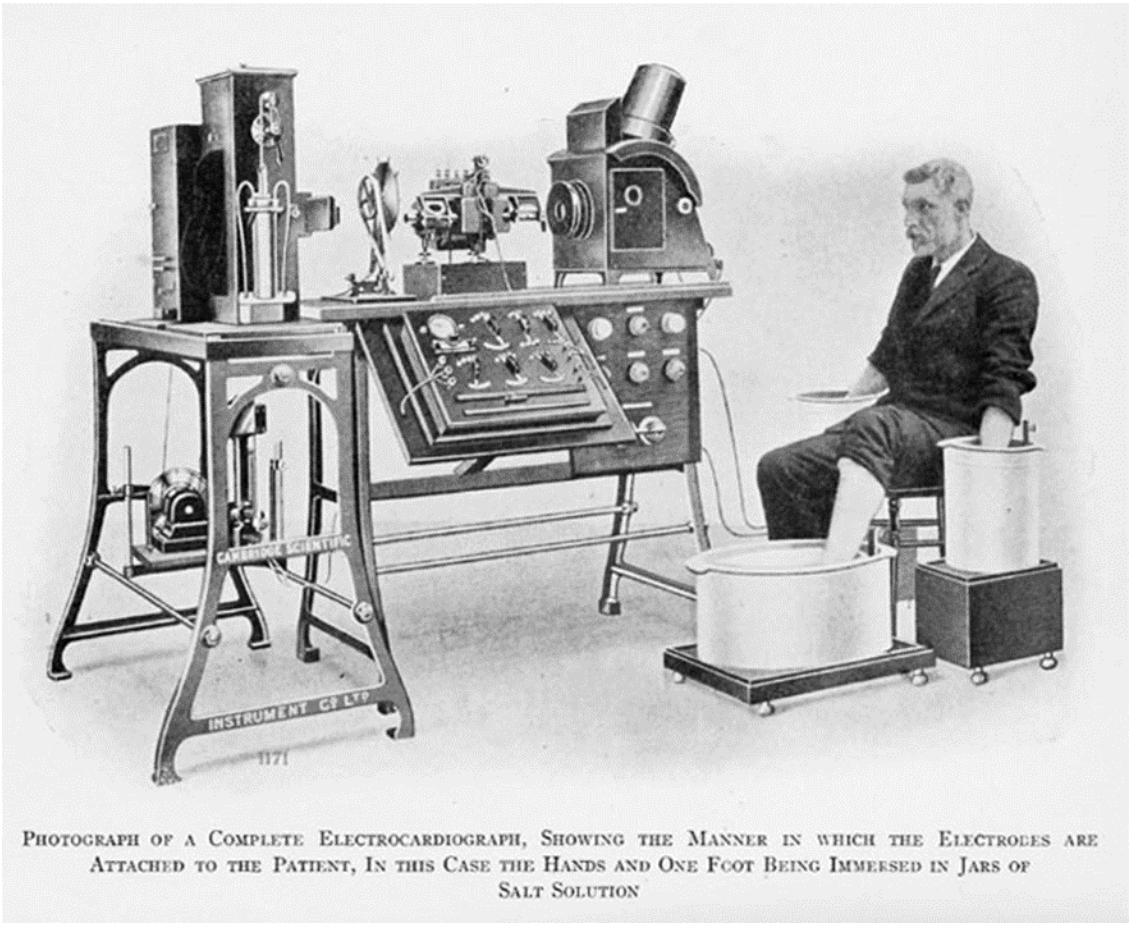

PHOTOGRAPH OF A COMPLETE ELECTROCARDIOGRAPH, SHOWING THE MANNER IN WHICH THE ELECTRODES ARE ATTACHED TO THE PATIENT, IN THIS CASE THE HANDS AND ONE FOOT BEING IMMERSED IN JARS OF SALT SOLUTION

Figure 4. An early commercial ECG device (1911)

Alexander Muirhead is reported to have attached wires to a feverish patient's wrist to obtain a record of the patient's heartbeat in 1872 at St Bartholomew's Hospital [47]. It has been more than one hundred years. With the continuous advancement of science and technology, many advances in electrocardiography have been made over the years. An initial breakthrough came when Willem

Einthoven, working in Leiden, the Netherlands, used the string galvanometer (the first practical electrocardiograph) he invented in 1901 [23]. In 1937, Taro Takemi invented a new portable electrocardiograph machine [24]. From the early commercial ECG device as shown in Figure 4, improved to the hospital ECG monitor and the 24-hour Holter ECG device. Nowadays, wearable devices have become popular.

ECG devices are improving smaller and smaller. However, these devices still have some inconveniences during using. It is necessary that electrodes are attached to the body during using the hospital or Holter ECG monitoring device. Even a wearable smartwatch needs to be touched by hand when collecting ECG data. The unconscious, unrestrained, and noncontact biosignal collection scheme is the trend and direction of future healthcare monitoring and management at home.

For most Japanese people, bathing is a part of daily routine. In addition to the daily cleaning, bathing also can be used as a scheme of healthcare monitoring at home. The unconscious, unrestrained, and noncontact biosignal collection can be achieved during daily bathing. However, there is a risk during bathing. Figure 5 shows the transition of drowning number in domestic bathtub from 2004 to 2018 according to statistics from the Ministry of Health, Labour and Welfare of Japan. The number is 5536 in 2017 and increased to about 2 times compared to 2,870 in 2004. Security monitoring can also be implemented during bathing. Biosignals monitoring during bathing can achieve not only unrestrained healthcare monitoring but also a bathing safety guarantee.

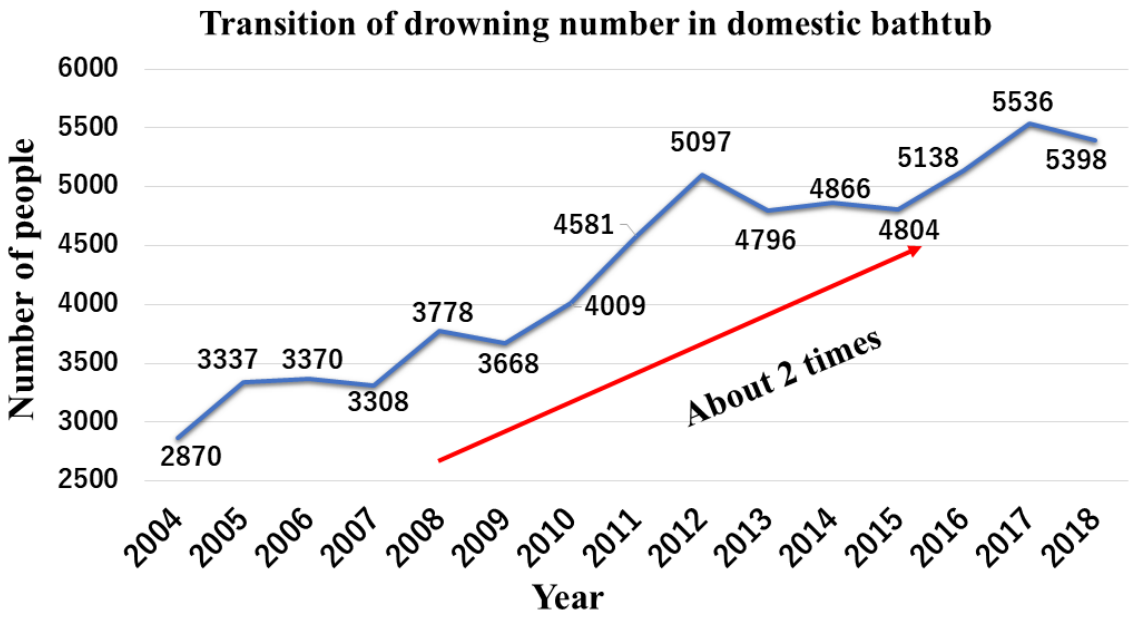

Figure 5. Transition of drowning number in domestic bathtub

Home healthcare management has gradually become ubiquitous, and bathtub ECG is an indispensable part of it. The bathtub ECG system has its own unique advantages in all methods of ECG acquisition. Bathtub ECG system typically uses noncontact electrodes to collect ECG signals. The noncontact electrodes reduce the discomfort of the subject compared to the contact electrodes. The data acquisition method is made more convenient by the unconscious data acquisition method of the bathtub ECG system. Ogawa et al. used the bathtub ECG signal for personal identification and the result showed that more than 91% of ECG data could be identified correctly among a family of five members [50]. Kawarada et al. designed a fully automated monitoring

system of health status in daily life that integrated with three monitoring devices of body and excreta weight in lavatory, ECG in bathtub and ECG in bed, and demonstrated the system are useful and helpful to measure the daily physiological information unconsciously in the young and elderly subjects [51]. Compared with conventional ECG collection, bathtub ECG is more convenient for health monitoring at home.

1.4 Stress Monitoring

There are two kinds of stress, including acute and chronic stress. Acute stress is the immediate response to a stressor. Chronic stress is the state caused by a constant stress stimulus [52]. Many changes in the body are triggered because the stress response is activated. These changes are caused by stimulation of SNS and inhibition of PNS. The heart rate, the blood supply to the muscles, respiratory rate, skin temperature, and cognitive activity increase, among several other responses. The biomarkers affected by the stress response are commonly used to evaluate or monitor stress [3,11,53].

Stress can be evaluated subjectively through questionnaires. It is the standard clinical practice. Stress also can be evaluated objectively by measuring various responses of the body to stress [54]. The most common methods in clinical stress evaluation are based on self-reported questionnaires such as Cohen's perceived stress scale, and self-reported visual scales such as the visual analogue scale for stress. Using biochemical markers to detect stress is more attractive for biomedical researchers, such as cortisol and α-amylase [55]. The subjects' stress states are triggered based on the Trier Social Stress Test [56]. There are multiple studies for stress evaluation using measuring biosignals of the body in response to stress [57].

Biosignals can be divided into two main categories, including physical signals and physiological signals [58]. Physical biosignals include respiration,

facial expressions, voice, pupil size, eye movements, blinks, et al. Physiological signals include ECG, EEG, EMG, et al. Evaluating stress based on EEG, the decrease of alpha and the increase of beta activity provide reliable estimators of stress [59].

In this dissertation, a bathtub ECG monitoring system is used to collect ECG signals during bathing. The bathtub ECG monitoring system is optimized. The most suitable electrode for bathtub ECG collection during bathing is selected based on the evaluation of the ECG signal quality. Using HRV analysis to estimate the optimal bathing time, combined with the stress index, the effect of stress on the optimal bathing time is obtained. Stress has an obvious effect on optimal bathing time. Stress increases the optimal bathing time. In high-stress situations, it takes longer to achieve the comfort of bathing. Bathtub ECG as a potential alternative to light stress test in daily life is proposed. The correlation between bathing and EST is explored. The relationship between bathing duration, water temperature, and the EST stage is analyzed. Daily bathing can serve not only for cleaning and healthcare monitoring but also as a reference for an at-home alternative to the EST.

Chapter 2

Effect of Stress on Optimal Bathing Time

It is common for Japanese people to take bathing in daily life. According to reliable research, over 80% of respondents said that they like to take a bath [60]. Daily bathing can clean the skin and promote the body's metabolism, which can bring relaxation to the body and mind, and contribute to physical and mental health. However, bathing has a risk for seniors and patients. Seniors generally decline physical and mental functions and environment self-adaptability during bathing, so the bathroom becomes a place where accidents are likely to occur. The number of drownings in a domestic bathtub was 5,536 in 2017 and increased to about 2 times over 13 years compared to 2,870 in 2004 [61]. Therefore, it is indispensable to perform biological signal monitoring during bathing. Moreover, the stress problem is getting worse in Japan. Consequently, the effect of stress on the optimal bathing time is explored in this study.

2.1 Data Collection

In this study, a noncontact bathtub ECG monitoring system was used to collect ECG signals during bathing. Figure 6 shows the scheme of the bathtub ECG monitoring system. The noncontact electrodes used in the bathtub ECG monitoring system were made of thin stainless-steel plates. The stainless-steel plate was fixed in a plastic case with a rubber, as shown in Figure 7. The dimensions of the stainless-steel plates were 120 mm × 45 mm × 0.3 mm and the specific gravity of the stainless-steel plates was 7.93. The dimensions of the plastic cases were 125 mm × 70 mm × 37 mm. There were three noncontact electrodes attached to the inner wall of the bathtub. The first one electrode was on the right side of the right arm as the negative of lead II ECG. The second one was on the side of the left leg as the positive of lead II ECG. The last one was on the side of right leg as the ground.

The participant sat in a relaxed position during bathing as shown in Figure 6. Lead II ECG signals were measured at a sampling rate of 500 Hz. The collected ECG signals were recorded in the data recorder (NF handy data recorder EZ7510, NF Corporation, Yokohama, Kanagawa, Japan) after amplifying. The ECG data were transferred to the personal computer through the universal serial bus (USB) cable and stored on the computer for processing and analysis.

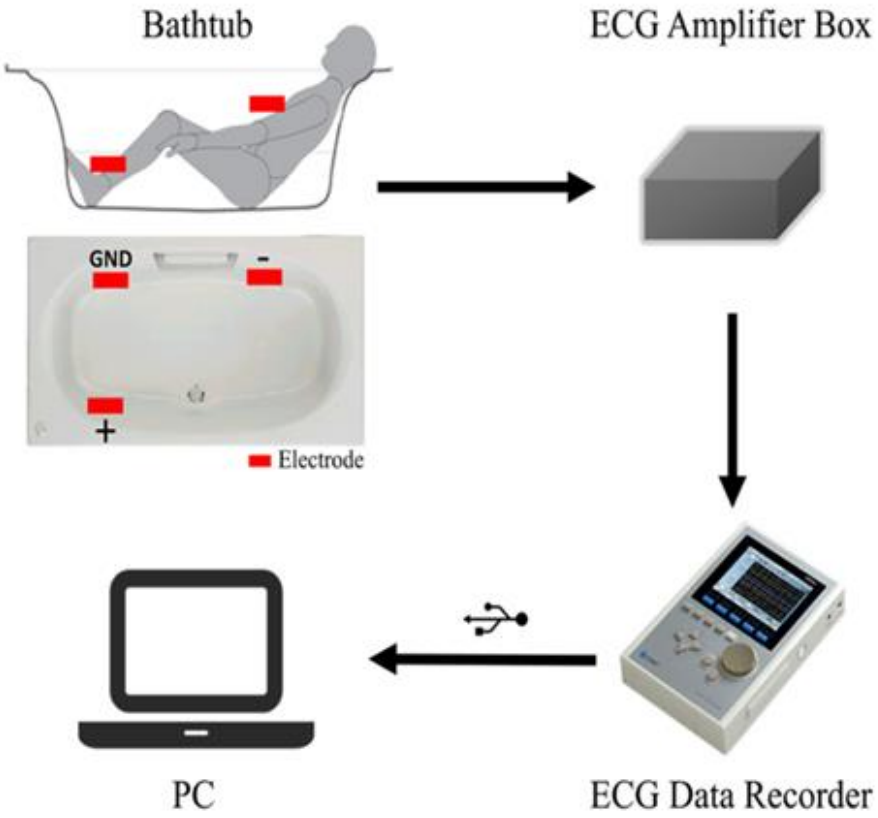

Figure 6. Scheme of the bathtub ECG monitoring system

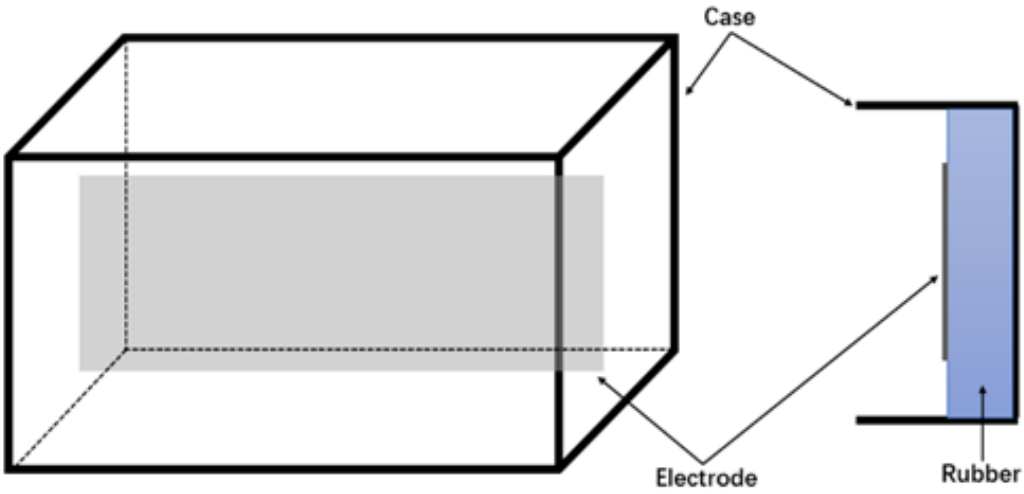

Figure 7. Electrode attached on bathtub wall

One healthy male participant was enrolled in the experiment. Informed consent was obtained from the participant before data collection. The participant was at the fifties without cardiac disease. ECG data were measured during his bathing on a daily basis over one year. Daily data acquisition begins after the participant had finished the day's work in the evening. The water temperature was set at 39 Celsius degrees (℃). The bath time was controlled in 15 minutes. Participant's physical indexes before and after bathing were measured and recorded in the working diary, including blood pressure (BP), HR, body temperature (BTp) and body weight (BW). Changes in the bathroom environment before and after bathing were also measured and recorded in the working diary, including temperature and humidity. The water temperature in the bathtub and the working and living conditions of the participants on the day were also recorded in the working diary. The participant's working diary was taken as a reference for the study.

2.2 Data preprocessing

The preprocessing included two steps: noise suppression and R-peak detection. Raw ECG signal was first decomposed into seven levels by multilevel one-dimensional wavelet decomposition. The final approximation coefficients were taken as the baseline drift and were subtracted from the original signal. Then,

a notch filter and a low-pass filter were implemented to remove power-line noise and high frequency (HF) distortions to achieve noise suppression. After noise suppression, R-peaks were detected and RRIs were calculated. Error detections or irregular heartbeats (arrhythmia, etc.) were removed as outliers. Figure 8 shows an example of one minute ECG signal before and after preprocessing.

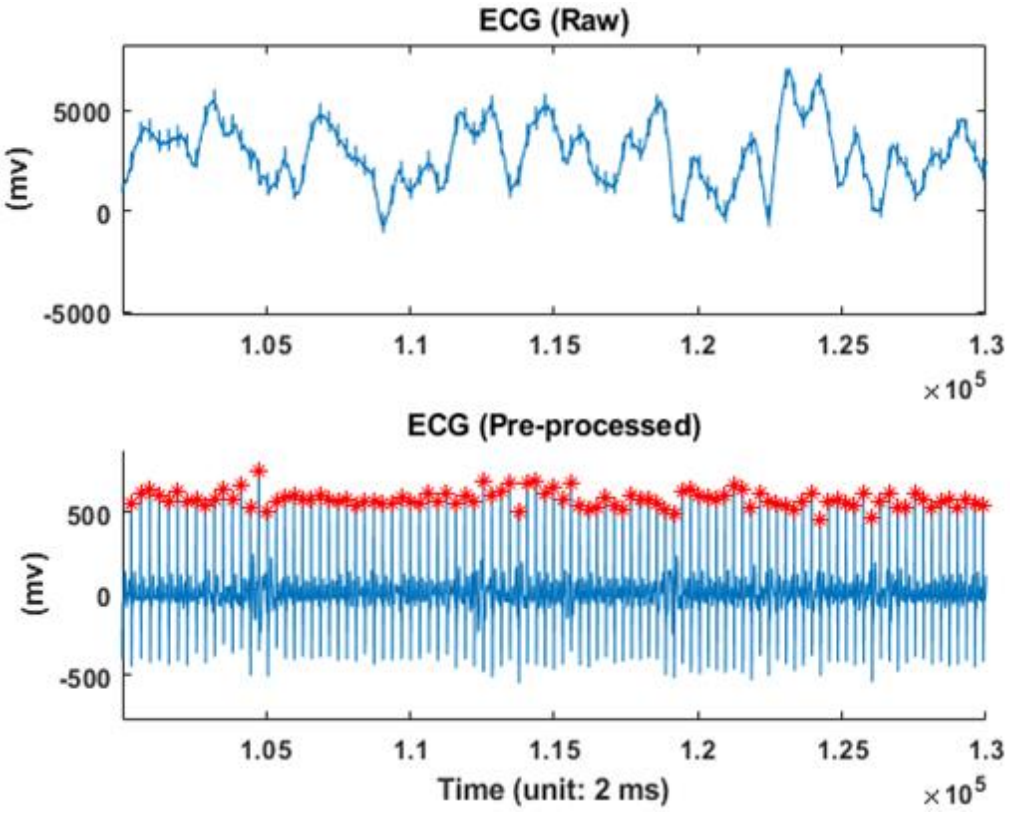

Figure 8. An example of one minute ECG signal before and after preprocessing

2.3 Stress Index Calculation

In previous studies, HRV features in time domain, frequency domain, and nonlinear domain were extracted for stress index (SI) calculation function, which consisted of four HRV features: root mean square of successive N-N interval (NNI) differences (RMSSD), normalized HF power (HFnu), sample entropy (SampEn), and noise limit (NL) [62].

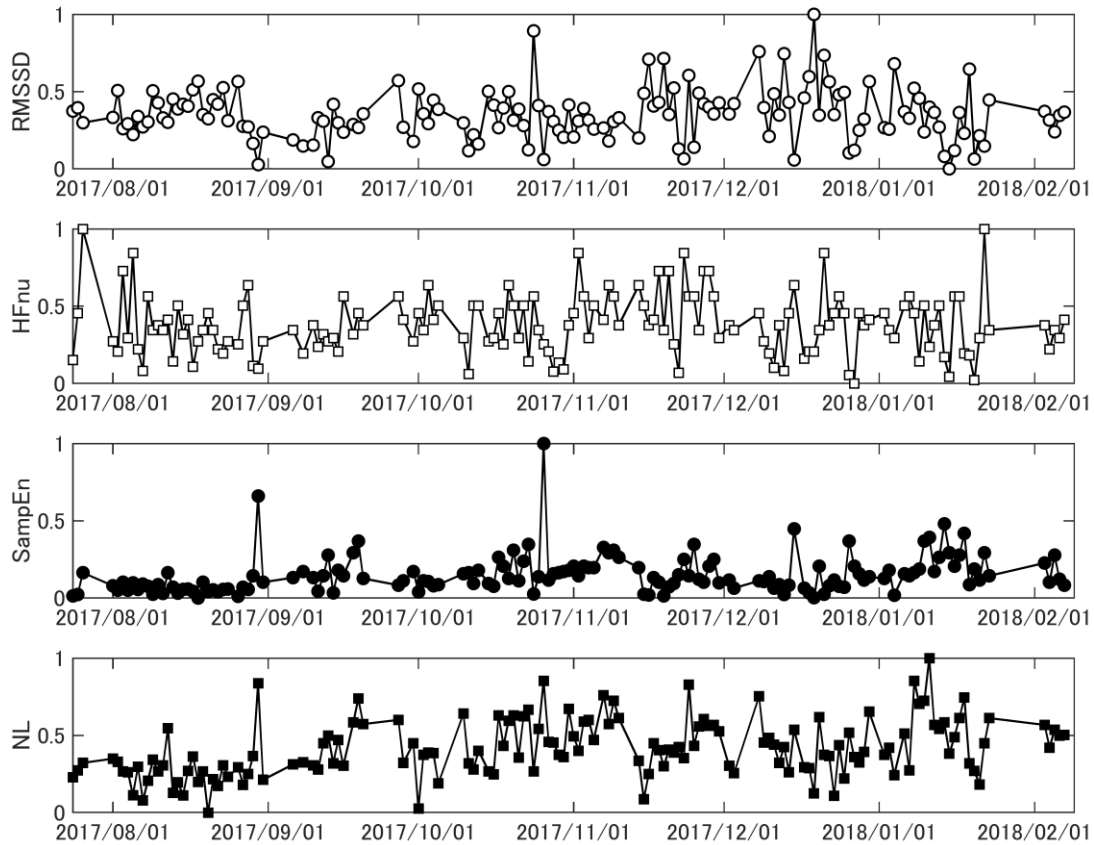

Figure 9. The variations of HRV features over six months

There is a consensus, among the different studies, that RMSSD and HF decreased during acute mental stress [63]. Reduced irregularity is also reported during stress condition [64]. The values of SampEn and NL can provide relative measures of nonlinear intensity [65], [66]. As shown in Figure 9, used HRV features are negatively correlated with stress. All features are calculated from 15 min NNI data.

HF: Power spectral analysis is applied to NNI data using an autoregressive model. The high frequency component (HF: 0.15 ~ 0.4 Hz) is estimated.

RMSSD: Detailed formula of RMSSD is shown by the following equation:

$$RMSSD = \sqrt{\frac{1}{n-1}\sum_{i=2}^{n}[NNI(i) - NNI(i-1)]^2}$$

where n is the data length, and i is the ith data point of NNI series.

Sample entropy: SampEn provides a generalized measure of complexity in a time series [65]. Lower values of SampEn indicate more self-similarity in the time series. Conversely, higher values of SampEn indicate greater irregularity and complexity in time series data. SampEn values can be calculated by:

$$SampEn(m, r, N) = -ln\left[\frac{A^m(r)}{B^m(r)}\right]$$

where N is the length of the input NNI series, and r is the tolerance for accepting matches. Bm(r) is the probability that two sequences will match for m points, whereas Am(r) is the probability that two sequences will match for m+1 points. In this study, a SampEn index is used with an embedded dimension (m) of 4 and

a tolerance (r) of 0.15.

Noise limit: Noise titration is a technique to identify the determinism of a short time series even in the presence of significant noise contamination [66]. In essence, this approach is analogous to a chemical titration process: incremental amounts of noise are deliberately added as a contrasting agent for nonlinearity. A discrete Volterra–Wiener–Korenberg series is used to model the predicted time series data. The nonlinear determinism is indicated if the best nonlinear model provides a significantly better fit to the data than the best linear model at the 1% significance level. Afterward, the indicator called the NL is calculated as the percent of signal power added as noise to "titrate" the data to the point of neutrality. Under this scheme, nonlinearity is indicated by NL > 0, and the value of NL provides a relative measure of nonlinear intensity.

SI was computed using the reciprocal of selected HRV features because they were negatively related to the stress level. The reciprocal of HRV feature was firstly normalized by:

$$Z = \frac{x^{-1} - min(x^{-1})}{max(x^{-1}) - min(x^{-1})}$$

where x is the HRV feature, Z is the normalized value of the HRV feature. Then, SI was calculated by the formula as follows:

$$SI = Z_{rmssd} \times Z_{hf} \times Z_{sampen} \times Z_{nl}$$

The bathing ECG data were classified into two sorts, one with low SI value during off days and another one with a high SI value, extracted for analysis of optimal bathing time.

Bathing ECG data during off days with low SI and without events were extracted for reference. The standard deviation of all NNIs (SDNN) per minute was calculated. The large SDNN value indicates that the HRV signal was highly complex. the HRV signal of healthy people was irregular and complex. Conversely, the SDNN small indicates that the HRV signal was simpler, indicating that the health status was not good. When the HRV drops significantly, it indicated that the body was in a state of disease. [30,34] Therefore, It was defined that the derivation of the optimal bathing time is the time of the SDNN's highest score when a graph was made that SDNN's value of every on time. However, the result of ECG data with low SI shows two sorts of waveforms had appeared, as shown in Figure 10. In pattern II, the SDNN after the first peak was less than the normal range, at this time the participant was under an uncomfortable state. Considering the age of the participant, the derivation of optimal bathing time was the time of the first SDNN's peak. Determining the optimal bathing time of high SI days by the same method, as shown in Figure 11. The comparative analysis was completed with optimal bathing time between low SI and high SI days.

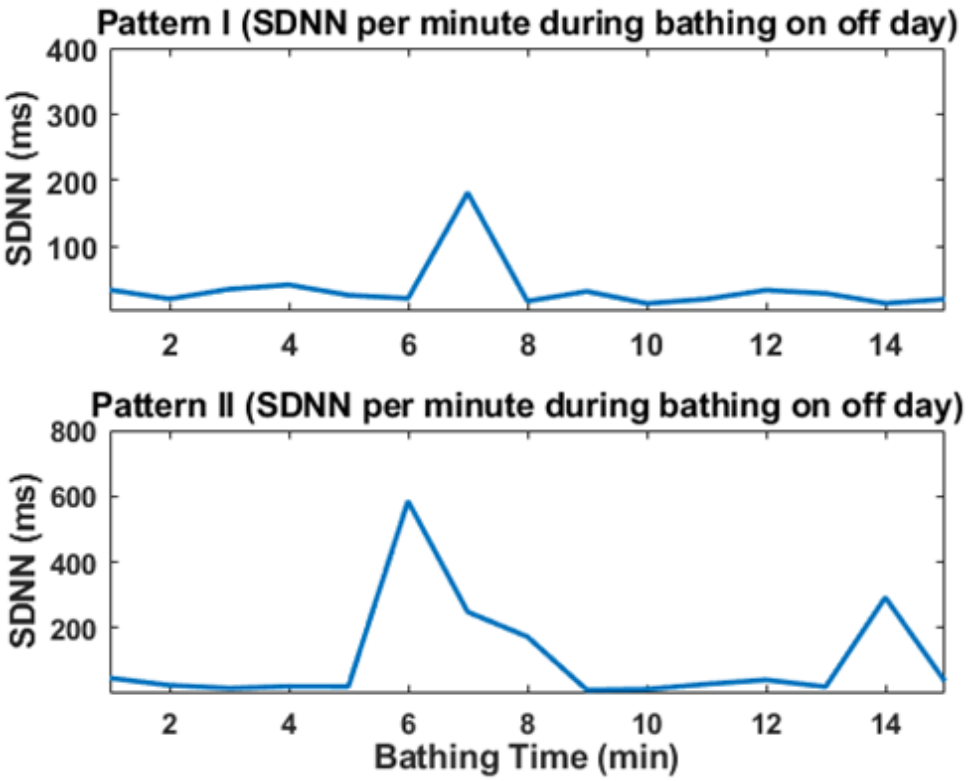

Figure 10. Pattern I and II of SDNN per minute during bathing on off day

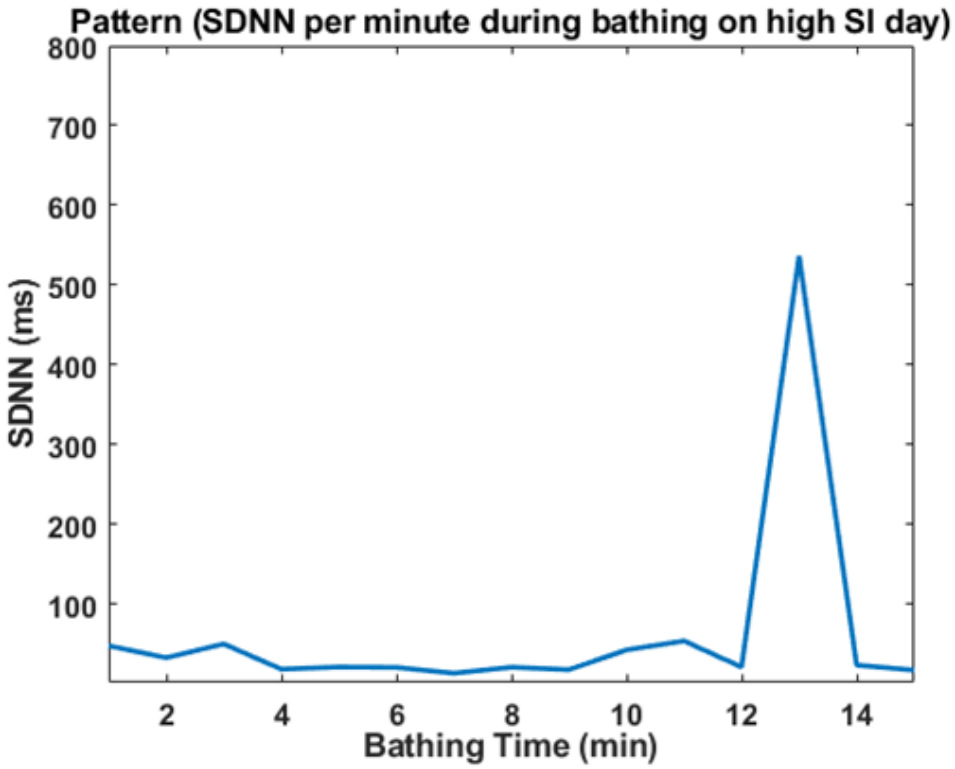

Figure 11. SDNN per minute during bathing on high SI day

2.4 Results

As shown in Figure 12 (a) – (d), the SI over one year was calculated to select the low and high SI days. Higher values of SI indicate higher stress, lower values indicate normal or relaxing conditions. Based on the value of SI and working diary, 30 high SI days and 40 low SI days were selected for analysis.

Figure 10 and Figure 11 show the different waveforms' sorts of SDNN per minute during bathing on off day and high SI day. There are two peaks of the SDNN value during the fifteen minutes of bathing in Figure 10. It indicates that the best comfort of bathing is achieved twice during bathing. And the periodic existence of the optimal bathing time is explained.

Figure 12. The variations of stress indexes over one year (a)

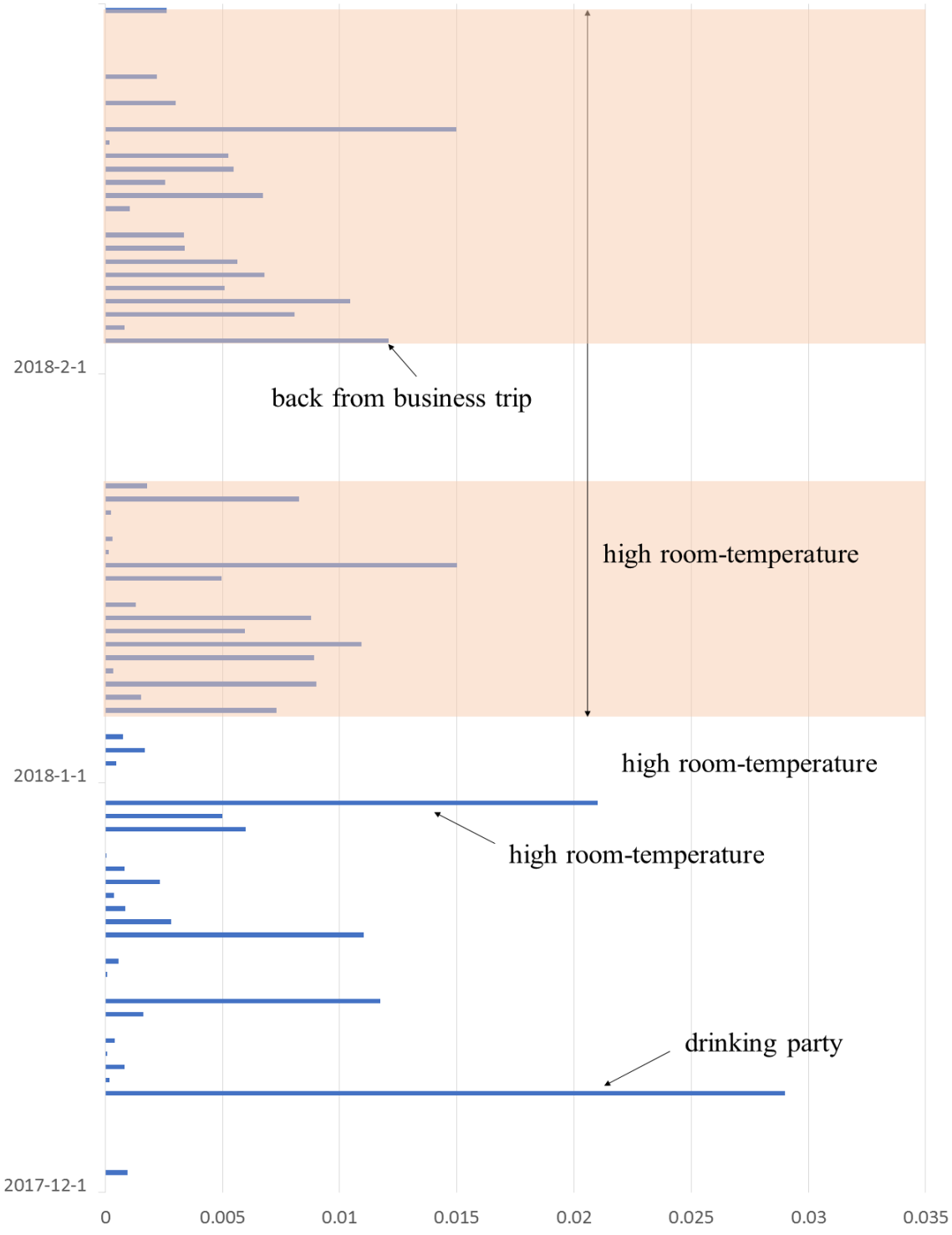

Figure 12. The variations of stress indexes over one year (b)

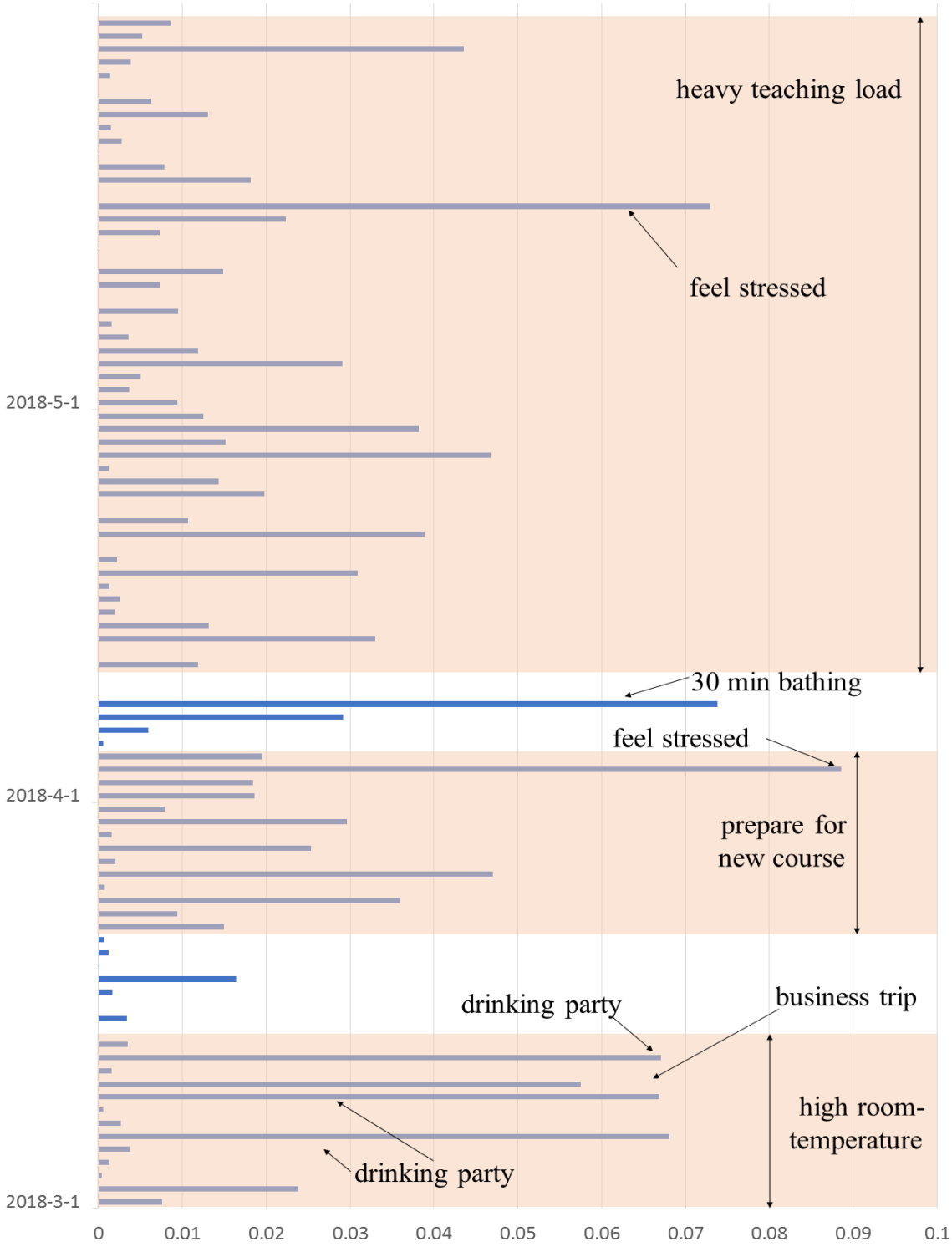

Figure 12. The variations of stress indexes over one year (c)

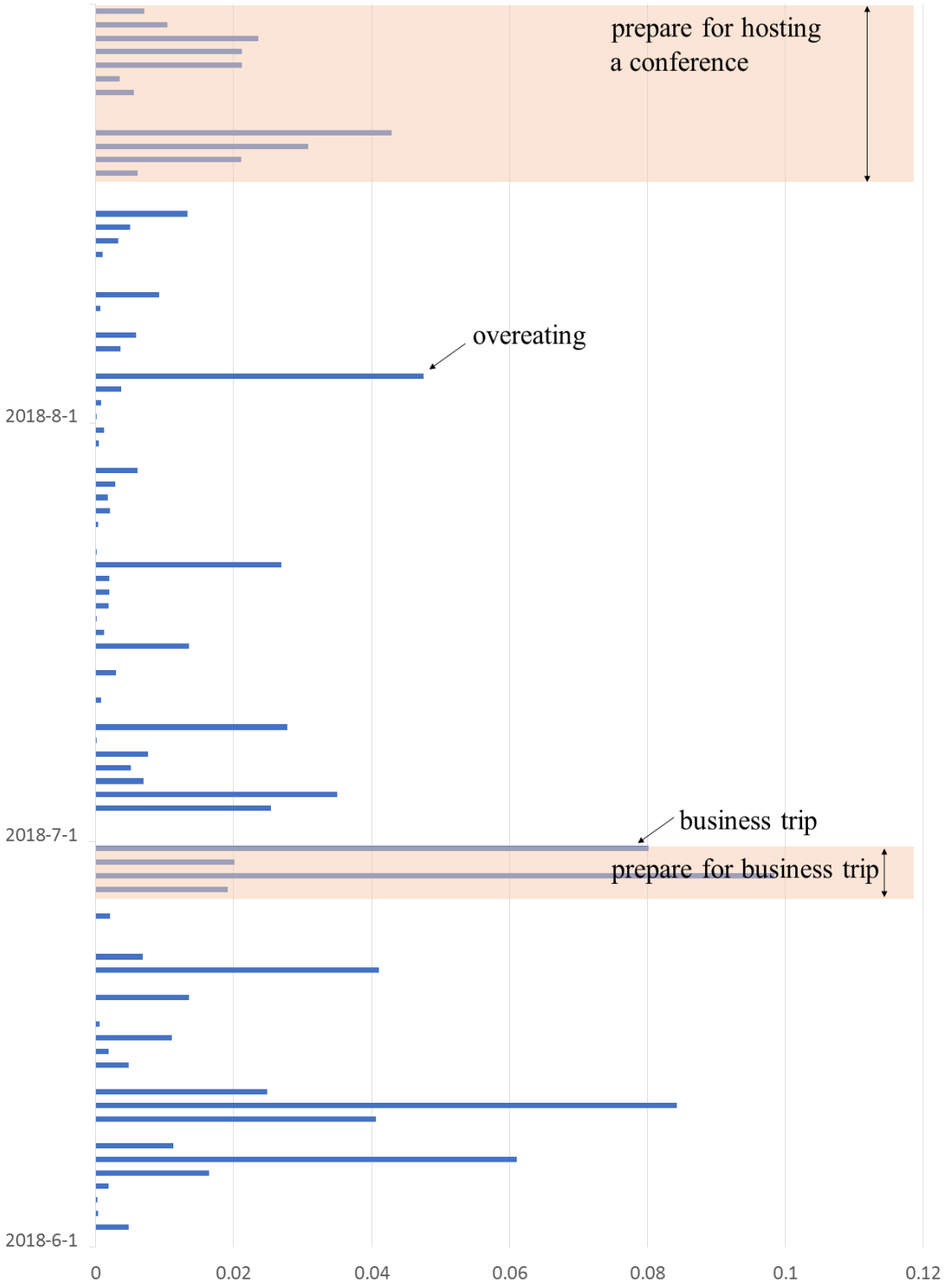

Figure 12. The variations of stress indexes over one year (d)

Figure 13 shows all the SDNN per minute during bathing on off days, and Figure 14 shows all the SDNN per minute during bathing on high SI days. It shows that the optimal bathing time on off days is within the first ten minutes of bathing, and the optimal bathing time on high SI days is within the last five minutes of bathing. The optimum bathing time is longer under high SI. It indicates achieving the best comfort needs a longer bathing time under high SI.

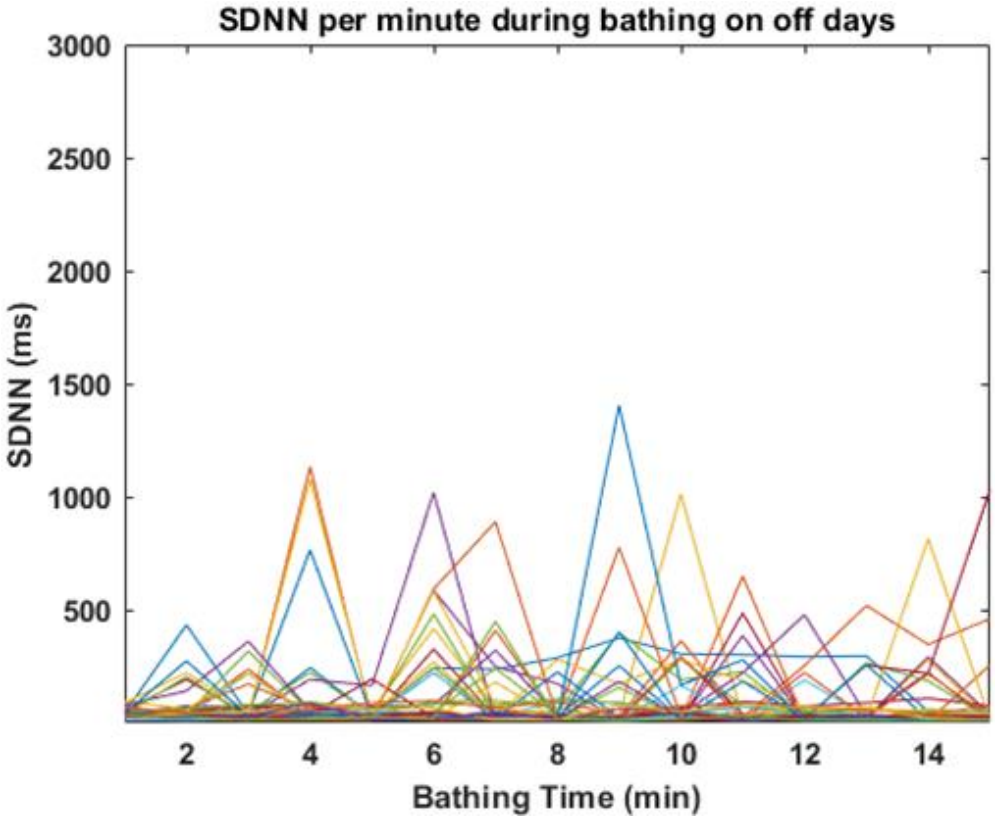

Figure 13. SDNN per minute during bathing on off days

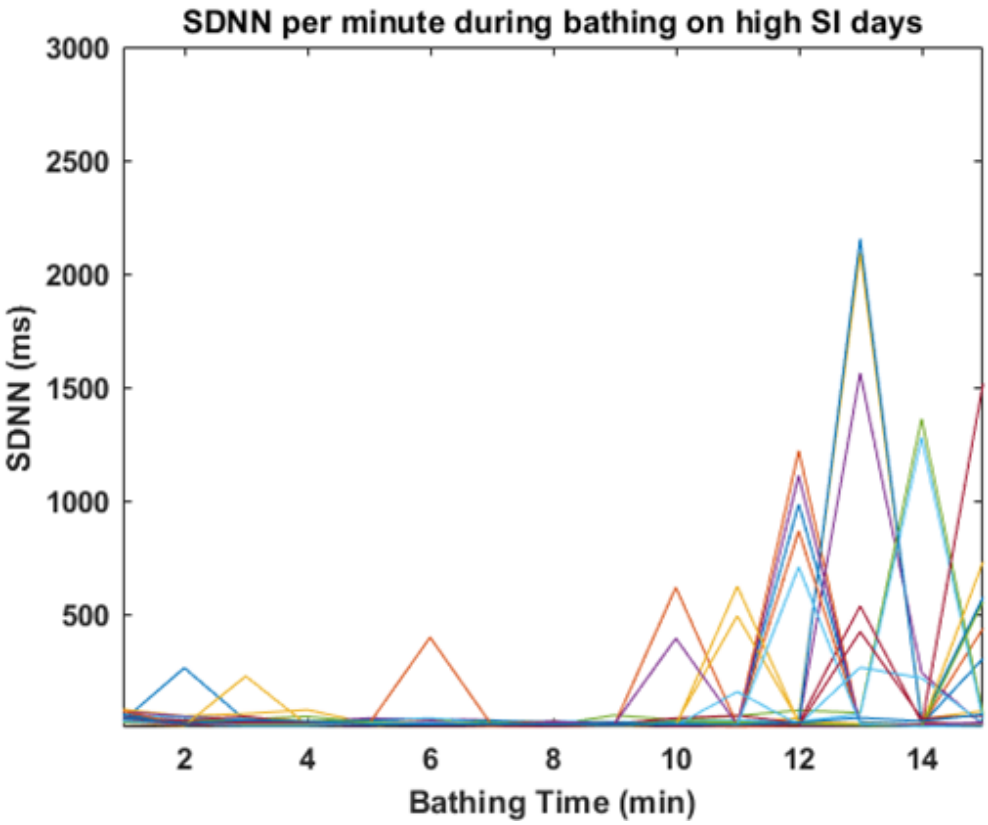

Figure 14. SDNN per minute during bathing on high SI days

Figure 15 shows the percentage of each optimal bathing time on off days. On off days, 87% of optimal bathing times are concentrated in 3 mins to 7 mins. Figure 16 shows the percentage of each optimal bathing time on high SI days. On high SI days, 82% of optimal bathing times are concentrated in 11 mins to 15 mins. The presence of stress severely delays the optimal bathing time.

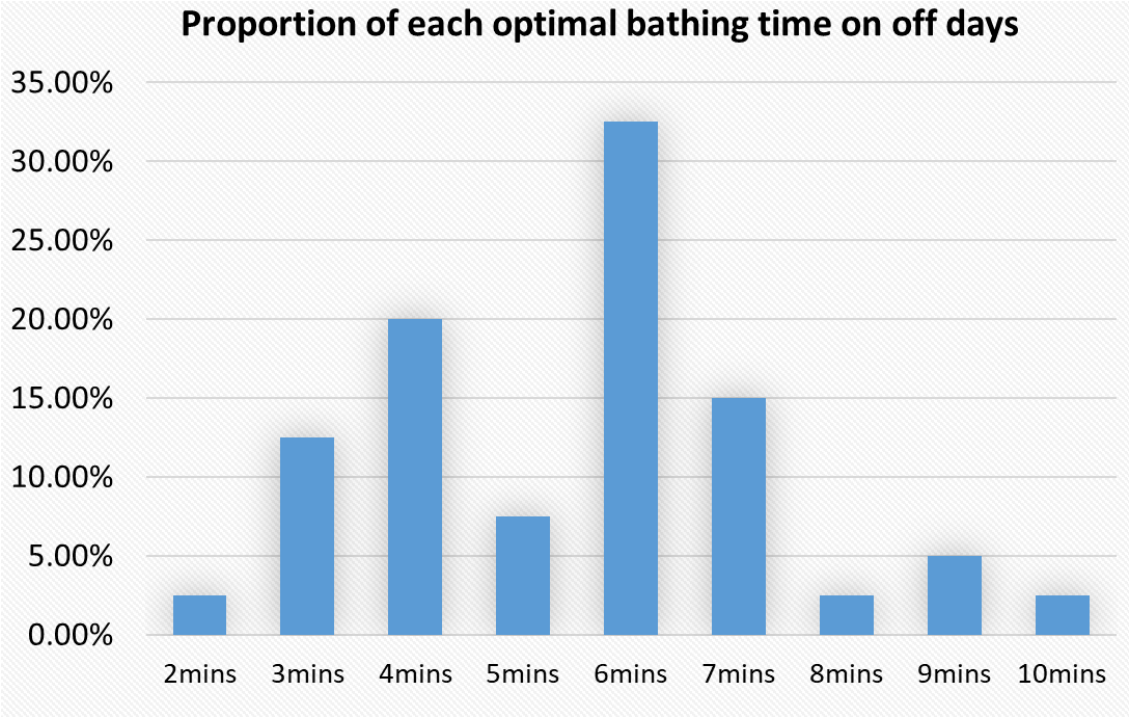

Figure 15. The proportion of each optimal bathing time on off day

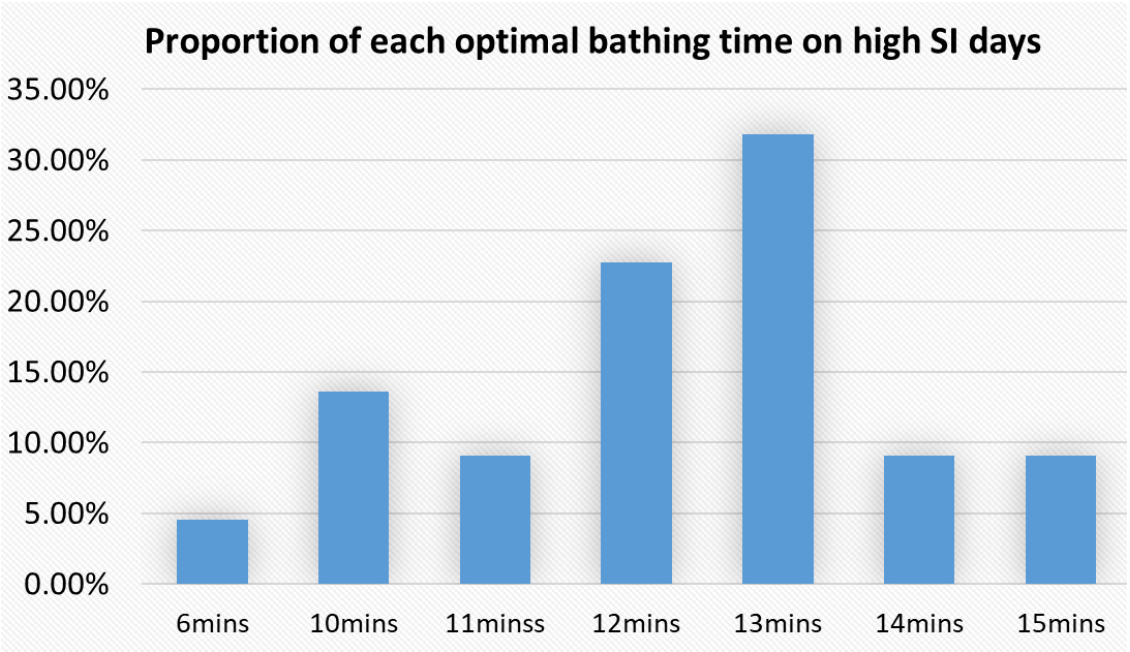

Figure 16. The proportion of each optimal bathing time on high SI day

2.5 Summary

In this study, the effect of stress on the optimal bathing time is explored. ECG signals are collected from one participant during bathing over one year. HRV analysis is completed after data preprocessing. SDNN is extracted to define the optimal bathing time. SI is calculated to determine the stress of each day. High SI days and off days are selected based on SI and working diary. Comparing the optimal bathing time of high SI day and off day, the optimal bathing time is longer on high SI day than on off day. The result shows that stress delays the optimal bathing time. Stress has an obvious effect on optimal bathing time. On the other hand, in high-stress situations, it takes longer to achieve the comfort of bathing. In future work, the extension of the bathing time is necessary to further verify the periodicity of the optimum bathing time. And participants of different ages and genders need to be increased to analyze the effect of stress on the optimal bathing time for different ages and genders.

Chapter 3

Bathtub Electrocardiogram Monitoring System

ECG is a common biosignal that can be collected during bathing [60,67,68]. In general, there are two non-contact approaches to collecting ECG during bathing. One uses direct contact of measurement electrodes on the inner wall of the bathtub with water [60,67]. Another uses the capacitive coupling electrodes placed outside the bathtub wall [69]. The valid ECG signals can be acquired with both methods, but there is a lot of noise in the acquired ECG signals.

There is a lot of noise during the acquisition and transmission of ECG. For example, power line interference, EMG noise, baseline wander, channel noise, electrode contact noise, motion artifacts, etc. [70,71,72,73,74]. In order to reduce the impact of these noises on data analysis, there are many methods to denoise during the data preprocessing before data analysis [70,71,73,75]. The noise in ECG during bathing is more than ECG in the case of using conventional conductive electrodes, mainly due to power line interference and movement of the bathing person [76]. In the study of bathing ECG, the collected ECG signals are greatly affected by the electrodes. But little research has focused on bathtub electrodes.

In this study, four different sizes of electrodes on the inner wall of the bathtub were used to collect the ECG signals during bathing. The performances of bathtub electrodes are assessed by estimating ECG signal quality. In the literature, some methods for assessing ECG signal quality are mentioned [77,78,79].

Several indices of ECG quality evaluation have been proved their effectiveness. Several indices of ECG signal quality assessment are used to assess the quality of ECG signals collected by electrodes of different sizes. The suitable bathtub electrode in the experiment is selected based on the performance of the electrodes.

3.1 Data Collection for Electronics Selection

A non-contact bathtub ECG monitoring system is used to collect the ECG signal. As shown in Figure 17, there are four sizes of non-contact electrodes (electrodes 1-4) attached to the inner wall of the bathtub. There are four electrodes of each size, for a total of sixteen electrodes. Four sizes of electrodes constitute an electrode group, as shown in Figure 17. The electrodes are stainless steel hemispheres with diameters of 50 mm, 32 mm, 25 mm, and 19 mm, and placed on the sides of the limbs. The electrodes and OpenBCI Cyton + Daisy

Biosensing Boards are connected with shielded cables. The OpenBCI Cyton Board and OpenBCI Daisy Module (which plugs into the OpenBCI Cyton Board) can be used to sample up to 16 channels of Electroencephalography (EEG), Electromyography (EMG), and ECG. The system communicates wirelessly to a computer via the OpenBCI USB dongle using RFDuino radio modules. It can also communicate wirelessly to any mobile device or tablet compatible with Bluetooth Low Energy (BLE). The CytonDaisy Board samples data at 125 Hz on each of its 16 channels.

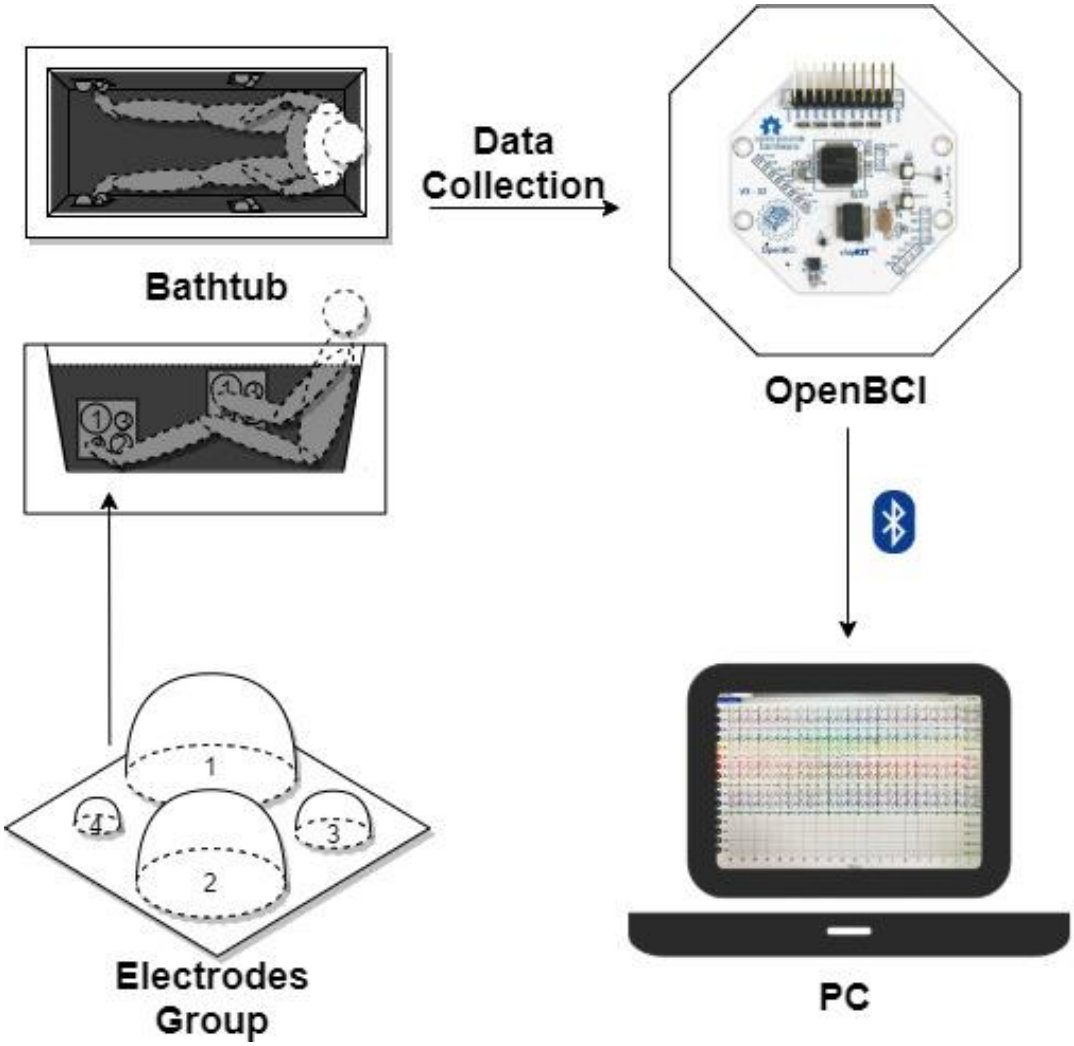

Figure 17. Non-contact bathtub ECG monitoring system and four sizes of electrodes

The participants sit in a relaxed position during bathing as shown in Figure 17. Limb leads (lead I, II, and III) ECG signals are measured at a sampling rate of 125 Hz. The ECG signals of 12 channels are collected simultaneously. And the ECG signals of 3 channels are collected via each size electrodes. The collected ECG signals are transferred to the computer through BLE and stored on the computer for processing and analysis.

Seven male participants are enrolled in the experiment. The participants are university students at twenties without cardiac disease. Informed consent is obtained from the participants before data collection. ECG data are measured once per participant during bathing. The water temperature is set at 39℃ and the room temperature is set around 27℃. The bathing time is controlled in 15 minutes. Physical indices of participants before and after bathing are measured and recorded in the experiment diary, including BTp, BW, and body height.

3.2 Signal Quality Index

In previous studies, the effectiveness of bathing ECG has been verified. After preliminary investigations, four signal quality indices (SQIs): kurtosis (kSQI), the relative power in the QRS complex (pSQI), principal component

analysis SQI (pcaSQI), and undetected error of R peaks (rSQI) are used to assess ECG signal quality [79,80]. The detailed information is as follows:

•*kSQI*

We segment each signal with the duration of 15 minutes to 180 signals with 5 s duration, then we calculate the kSQI of each 5s fragment and the equation of sSQI as follows:

$$kSQI = \frac{E\{X - \mu\}^4}{\sigma^4} - 3$$

•*pSQI*

Because the frequence of QRS complex is in the range of [5Hz, 15Hz], we hope a good quality ECG signal has the significant QRS complex. Thus, we calculate the energy ratio of QRS at the main frequency of ECG (5 Hz－40 Hz), the equation of pSQI as follows:

$$pSQI = \int_5^{15} P(f)\,df \;/\; \int_5^{40} P(f)\,df$$

When calculating pSQI, we need to remove baseline wander with a high-pass filter.

•*pcaSQI*

We use principal component analysis (PCA) to calculate the ratio of the first five eigenvalues over the sum of all eigenvalues of the signal with 15 minutes. For pSQI and pcaSQI, we use the average value of three leads (I, II, III).

•*rSQI*

Usually, R-peak is basic and important data in heart rate variability analysis. Whether calculating heart rate or analyzing in time- and frequency- domain, it starts from the RRI calculation. Therefore, the R-peaks detection is important from the collected ECG signals. The algorithm of Pan & Tompkins (TP) is used to detect R-peaks on the raw signals and denoised signals. Each 15 mins ECG signal is segmented into 90 signals with 10 s duration. After noise removal, the TP algorithm is used to find the number of R-peaks of each filtered 10 s signals, and the number is as the gold standard (N1). Next, the same TP algorithm is used to find the number of R-peaks of each 10 s signals without filtering (N2), after that, the difference between N1 and N2 is calculated. This difference is defined as undetected error of R-peaks (rSQI). For this index, three leads' signals are used to calculate the average detection error. And the number of R-peaks error detection is calculated.

All indices are calculated from 15-min ECG data.

3.3 Results

Figure 18 shows 10 s participant's raw lead I ECG signals of each size electrode. The ECG signal collected by electrode 1 has obviously more hum noise than other sizes. The ECG signal collected by electrode 3 has the least hum noise. The amount of noise in each segment signal can be intuitively compared.

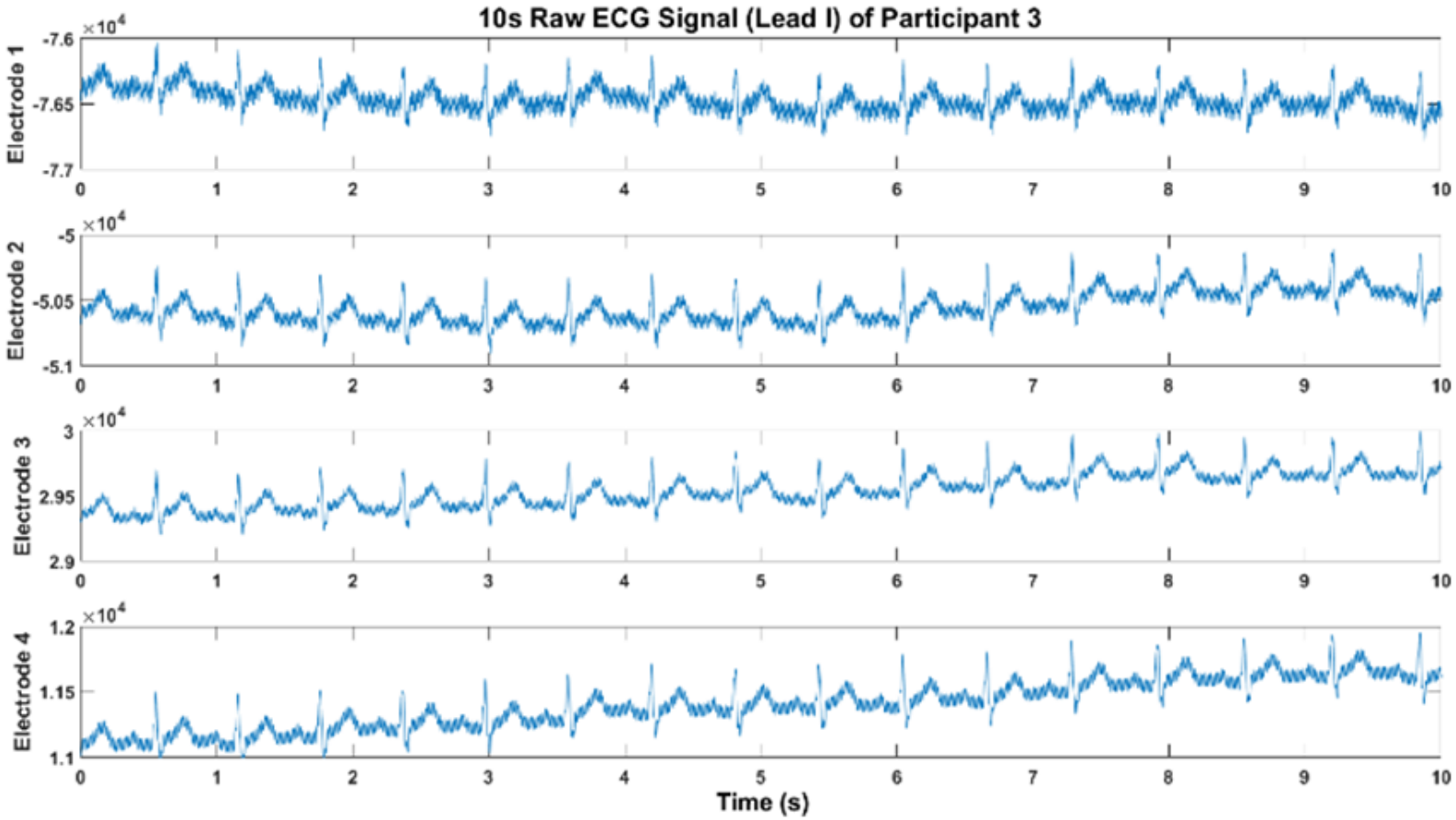

Figure 18. 10 s raw lead I Signals of each electrode

Figure 19 shows the kSQI of the four sizes electrodes for each participant. The kSQI values of participants 2 and 5 are smaller than the other participants. The kSQI values of electrode 1 for participant 1, participant 3, and participant 5 are larger than the other electrodes. The kSQI values of electrode 2 for participants 6 and 7 are larger than the other electrodes. The kSQI value of electrode 4 of participant 4 is larger than the other electrodes. The smaller the value of kSQI, the better the signal quality. Among the four size electrodes, the signal quality of electrode 3 is determined to be the best based on the value of kSQI.

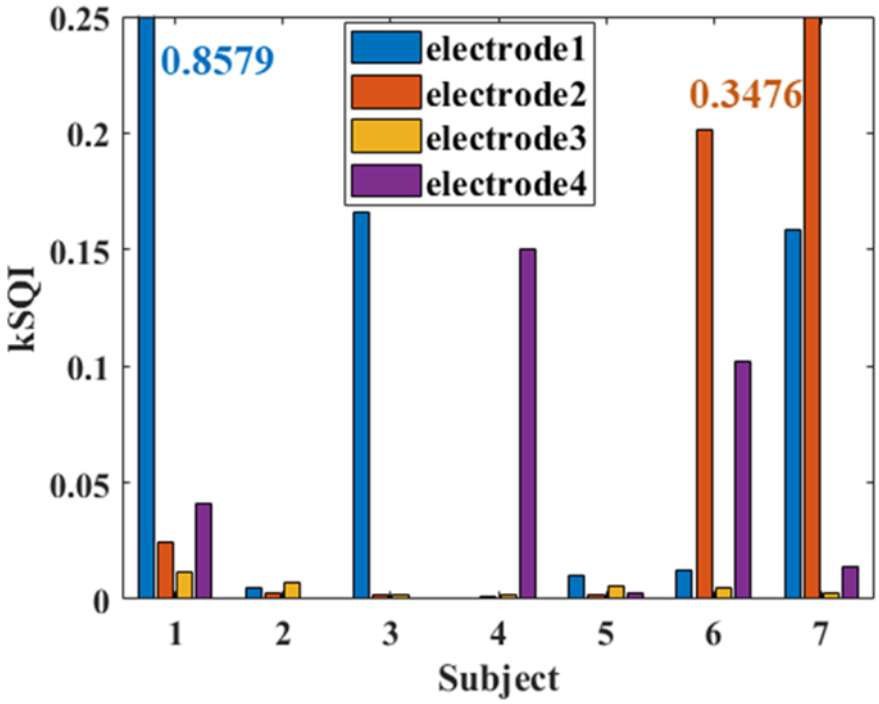

Figure 19. Absolute kSQI. The first electrode has an extreme absolute kSQI for subject 1, the second electrode also shows a maximum kSQI for subject7, the electrode 3 always keep a small and normal kSQI for the 7 subjects.

Figure 20 shows the results of pSQI of four sizes electrodes. The pSQI values of four sizes electrodes are between 0.45 and 0.8. The median of pSQI values for electrode 2 is the largest. The median of pSQI values for electrode 4 is the smallest. The larger the value of pSQI, the better the signal quality. Among the four size electrodes, the signal quality of electrode 2 is determined to be the best based on the value of pSQI.

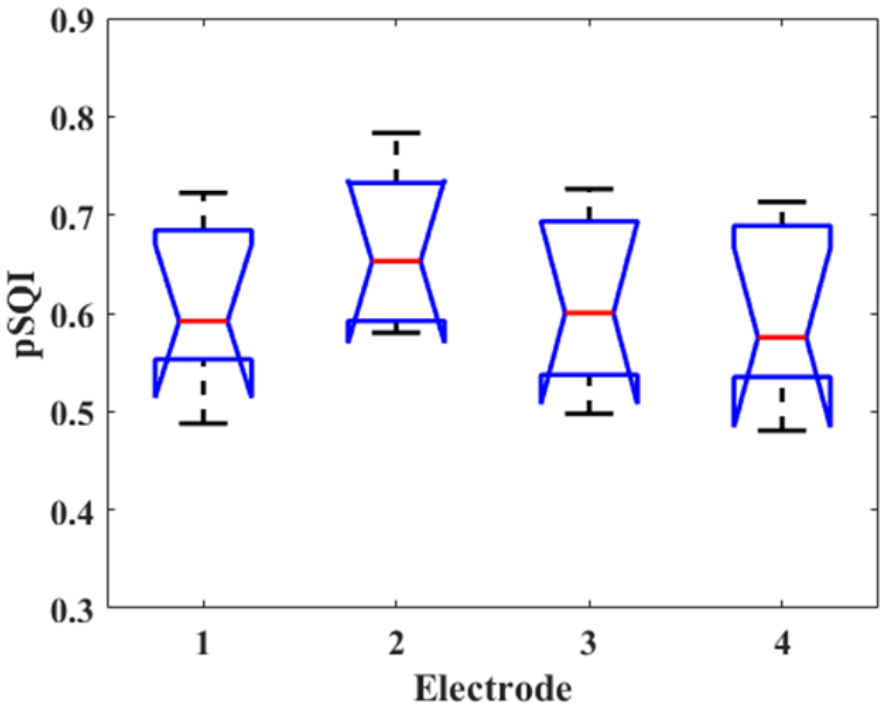

Figure 20. pSQI. Electrode 2 shows the highest pSQI, electrode1 and electrode3 almost have the same value about 0.6.

Figure 21 shows the results of pcaSQI of four sizes electrodes. The pcaSQI values of four sizes electrodes are between 0.72 and 0.92. The median of pcaSQI values for electrode 4 is the largest. The median of pcaSQI values for electrode 2 is the smallest. The larger the value of pcaSQI, the better the signal quality. Among

the four size electrodes, the signal quality of electrode 4 is determined to be the best based on the value of pcaSQI.

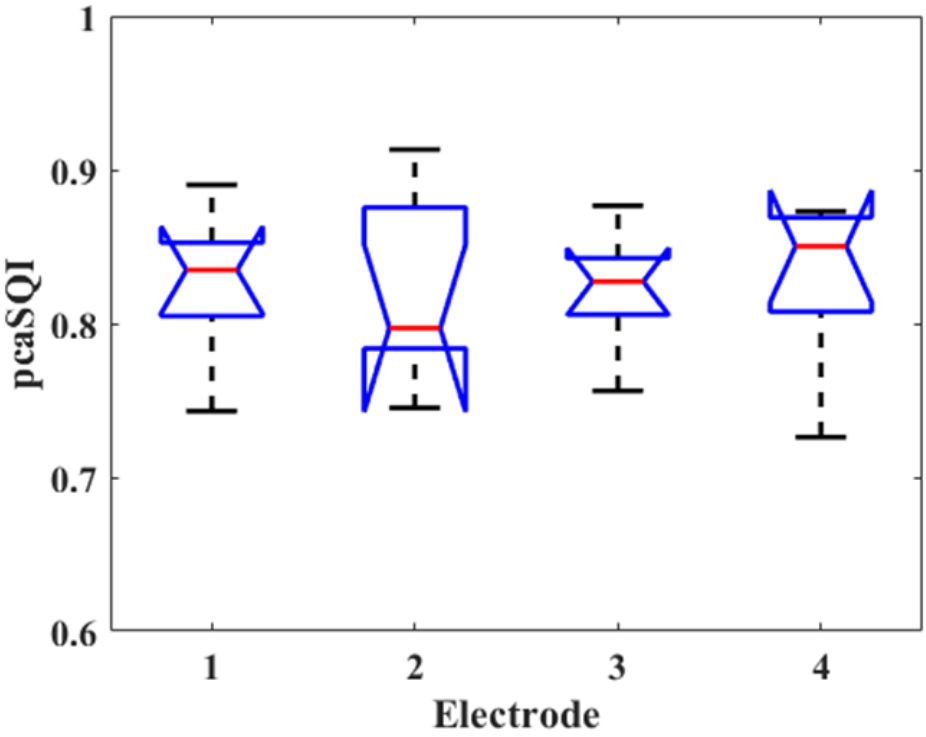

Figure 21. pcaSQI. Electrode 2 shows the smallest pcaSQI, the rest three electrodes almost have the same pcaSQI with about 0.85.

Figure 22 shows the rSQI of the four sizes electrodes for each participant. The rSQI values of participant 2 and 3 are smaller than the other participants. The rSQI values of electrode 2 for participant 1, 5, and 7 are larger than the other electrodes. The rSQI values of electrode 1 for participant 4 and 6 are larger than the other electrodes. The rSQI values of electrode 4 for participant 2 and 3 are larger than the other electrodes. The rSQI values of electrode 3 for participant 2,

4, 5, 6, and 7 are smaller than the other electrodes. The smaller the value of rSQI, the better the signal quality. Among the four size electrodes, the signal quality of electrode 3 is determined to be the best based on the value of rSQI.

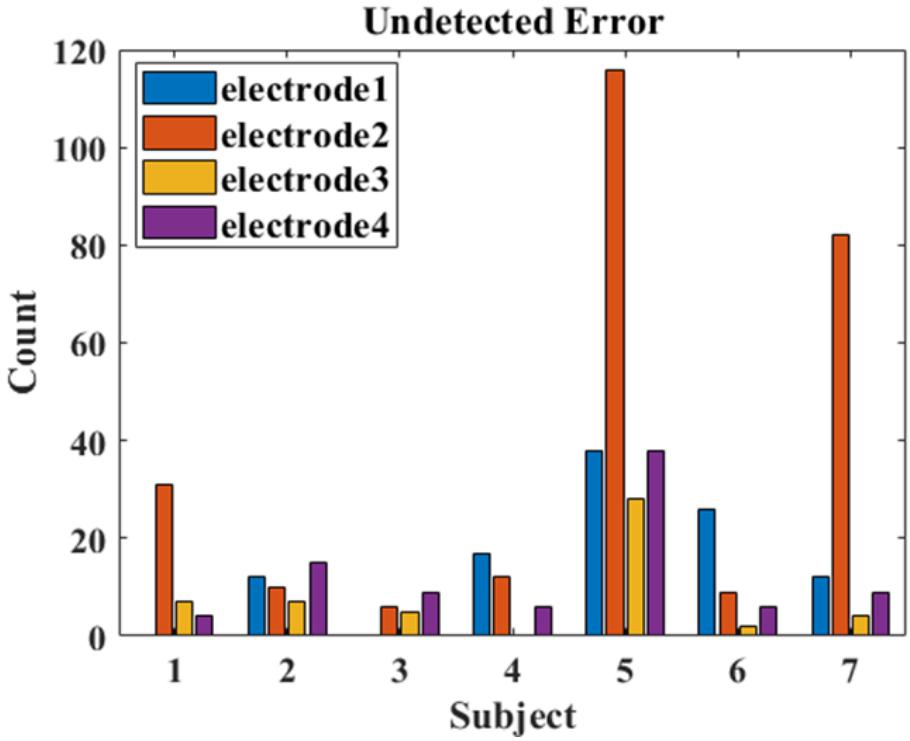

Figure 22. rSQI. Electrode 2 has an extreme undetected error value for subject 5 and subject 7, electrode 3 almost has the lowerest undetected error for each subject.

The result of performance evaluation of each size electrode in the four SQIs as illustrated in Table 4. The performance of electrode 3 is determined good two times in kSQI and rSQI. In pSQI, electrode 3 is determined the second level. Due to the experimental environment of the bathtub, small electrodes are more suitable. Therefore, electrode 3 is the most suitable electrode in this study.

Table 4. Performance evaluation of each size electrode in all SQI.

Evaluation / SQI	Good	←	←	Bad
kSQI	**3**	**4**	**1**	**2**
pSQI	**2**	**3**	**1**	**4**
pcaSQI	**4**	**1**	**3**	**2**
rSQI	**3**	**1**	**4**	**2**

3.4 Summary

The results obtained indicate that the performance of the four sizes electrodes for different indices is not consistent. The closer kSQI is to 0, the better the signal quality. pSQI and pcaSQI get higher value, the signal quality is better. The smaller value of rSQI, the higher the accuracy. The performance of electrode 2 is the best on pSQI, so the signal quality of electrode 2 is the best. But the performance of electrode 2 on pcaSQI is the worst. The performance of electrode 4 is the best on pcaSQI, so the signal quality of electrode 4 is the best. But the performance on pSQI is the worst. As shown in Figure 19, the kurtosis

of electrode 3 for each participant is close to 0. The signals quality of electrode 3 is the best based on kSQI. And the performance of electrode 1 is stable on pSQI and pcaSQI. As shown in Figure 22, the rSQI value of electrode 3 is the smallest, and the performance on each participant is stable. The performance of the four sizes electrode for different participants is not consistent. As shown in Figure 19, the performance of electrode 1 on participant 2, 4, 5, and 6 is better than on participant 1, 3, and 7. The performance of electrode 2 on participant 6 and 7 is worse than others. The difference in the performance of each electrode is not significant on pSQI and pcaSQI. However, it is easy to distinguish between good and bad based on kSQI and rSQI.

Combing the indices, the performance of electrode 3 is better and more stable. Considering that HRV analysis is essential in future study, electrode 3 is suitable based on the best performance of rSQI. Due to the experimental environment of the bathtub, small electrodes are more suitable. In summary, compared with other electrodes, electrode 3 is the most suitable for bathtub ECG collection in this study.

Chapter 4

Bathtub ECG as a Potential Alternative to Light Stress Test in Daily Life

The exercise stress test (EST) is a safe procedure as a common cardiological test that doctors use to diagnose coronary artery disease (CAD). The EST has been developed to apply widely so far, including evaluation of the anatomic and functional severity of CAD, evaluation of exercise-related symptoms, and assessment of the response to medical interventions [81]. In addition to the diagnostic value of screening cardiovascular disease, EST also has a significant prognostic value. Goldschlager et al. confirmed that EST can be used for diagnosing myocardial ischemia and CAD based on ESTs on 269 patients and 141 normal subjects [82]. Théroux et al. implemented a limited EST before hospital dis-charge of 210 patients after acute myocardial infarction and proved that this test is safe and can predict mortality in the subsequent year [83]. EST has also been used for valvular heart disease patients to quantify disability and

reproduce exercise-induced symptoms and assess responses to medical and surgical interventions [84]. There are multiple proto-cols for EST, the Bruce protocol is one of the most popular protocols [85]. It has been 59 years since the introduction of the Bruce protocol in 1963, and the protocol has developed from the first version of four stages to the modified Bruce protocol [86]. The EST is generally safe but there have been reports of myocardial infarction, arrhythmia, and deaths during tests, expected to occur once every 2,500 tests [87,88]. The EST should be implemented under the supervision of a physician [89]. Therefore, EST is not suitable for daily application.

In Japan, bathing is popular in daily life with many people and has become an al-most routine activity [60]. Multiple studies on bathtub ECG exist. Kwatra et al. proposed a different method from the conventional bioelectric measurement for recording ECG signals from a home bathtub setup [90]. Tamura et al. designed a bath-tub heart rate monitor and applied it in a fully automated monitoring system of health status at a pilot house [51,91]. Ogawa et al. completed identifying the bathtub ECG signal using a neural network with wavelet transform [50]. Mizukami et al. confirmed that a bathtub ECG is a suitable method to follow up patients with a pacemaker implanted [92]. Xu et al. confirmed that HRV using a bathtub ECG is impacted by water temperature during bathing [93]. In our previous study, the SI was calculated to evaluate daily stress using a bathtub ECG and using a convolutional neural network personal identification with a bathtub ECG [62,94]. A bathtub ECG is confirmed as convenient for collection and suitable for daily healthcare monitoring.

Exercise is one of many tolerable physiological stresses that can induce cardiovascular abnormalities that are not present at rest. In an EST, the most common exercise-induced stressor is an exercise on a treadmill or a bicycle ergometer. Sympathetic discharge is maximal and parasympathetic stimulation is withdrawn during strenuous exertion [95]. In bathing, the stressful load is from water pressure and thermal irritation. Gorman et al. identified sympathetic activation and parasympathetic withdrawal during thermal stress in a baboon [96]. There are potential shared mechanisms of action between thermal stress and exercise stress.

HRV is a reliable reflection of the many physiological factors modulating the cardiac rhythm [30]. Karthikeyan et al. used short-term ECG and HRV signals of the Stroop color word-based stress-inducing task to detect stress and achieved an overall average classification accuracy of 91.66% and 94.66% using probabilistic neural network algorithm and k-Nearest Neighbor (KNN) algorithm classifiers [97]. Munla et al. used a support vector machine with radial basis kernel function to complete driver stress detection based on HRV analysis and achieved an accuracy of 83% [98]. Ferdinando et al. used KNN to implement emotion recognition based on new features from short ECG signals and HRV features, and offered an approach to emotion recognition based on short ECG signals [99]. Orphanidou et al. proposed a quality assessment system based on wavelet entropy measurements of the HRV signal for wearable sensors [100]. Zarei et al. proposed an algorithm using new features extracted from HRV and ECG-derived respiration signals for the detection of obstructive sleep apnea [101]. In this study, HRV analysis is implemented to extract features of the EST

and bathing test (BT), using the features to investigate the HRV behaviors of the BT and EST for similarity.

The scheme of the implementation procedure of this study is shown in Figure 23. The ECG signals are collected during the EST and BT. Extraction of HRV features is implemented after raw signal denoising and R wave peak detection on preprocessing. The PCA is used for data dimensionality reduction of HRV features. The data after dimensionality reduction via the Voronoi diagram are used to evaluate the equivalent EST stages in terms of HRV behaviors of the BT. EST Stages 1–7 are grouped to low stage (Stages 1 and 2), medium stage (Stages 3 and 4), and high stage (Stages 5, 6, and 7) for investigating and evaluating the equivalent EST stage of the BT.

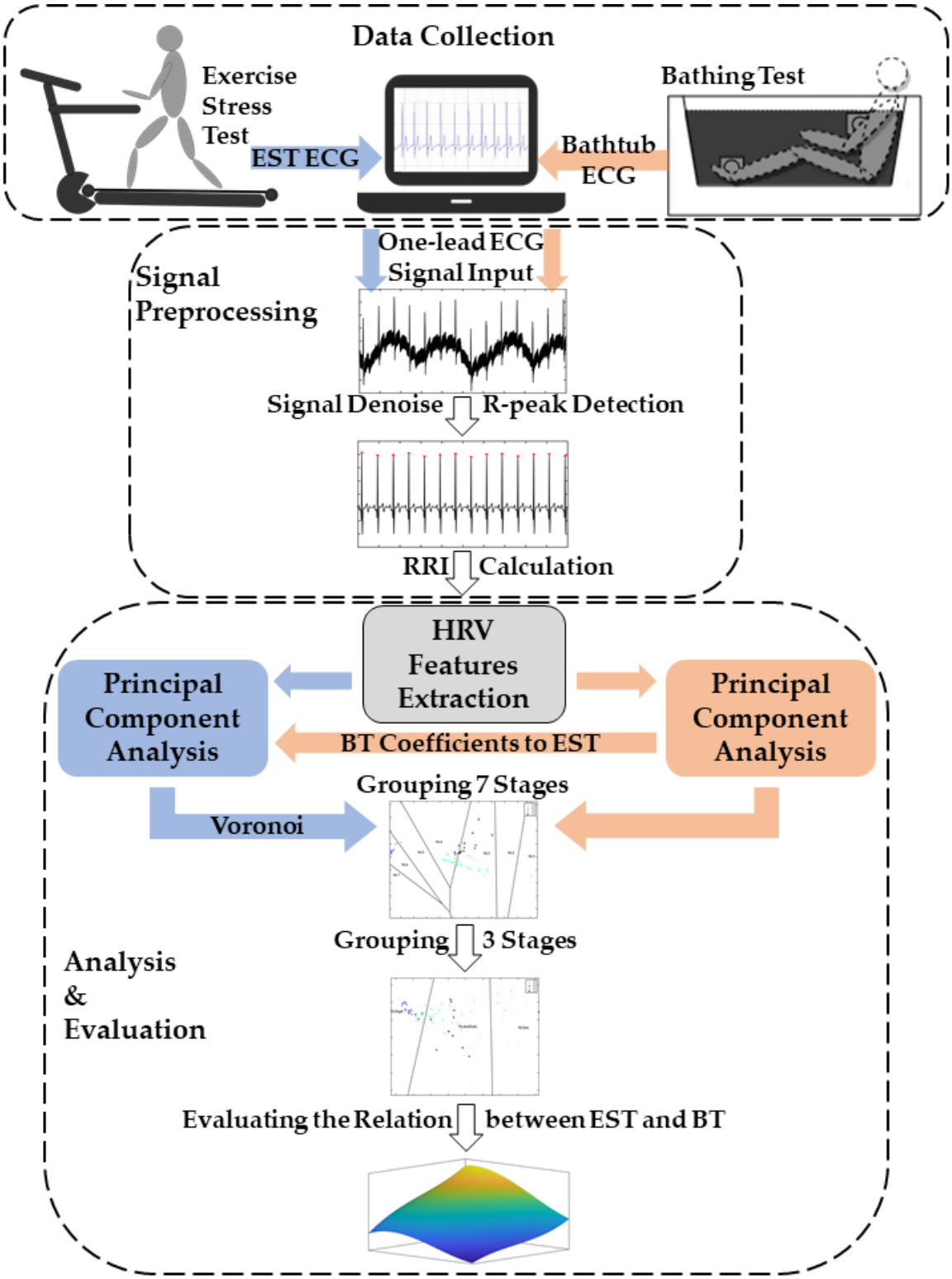

Figure 23. Scheme of the implementation procedure of this study. Blue arrows represent the EST. Pink arrows represent the BT.

4.1 Data Collection

Data collection consists of two parts in this study, including the BT and the EST. Ten healthy male subjects were enrolled in this data collection. All the subjects were university students in their twenties to thirties without cardiac disease. The data collection procedure was explained to subjects and written informed consent was obtained from all subjects before data collection. Basic information of subjects, including age, gender, body weight, height, and health status, was recorded in the experiment diary before data collection.

4.1.1. Bathing Test

A bathtub ECG monitoring system was built for data collection of the BT as shown in Figure 24. This system consists of three components: bathtub electrodes, an ECG monitoring device (OpenBCI Ganglion system, OpenBCI, Inc., Brooklyn, NY, USA), and a computer (MacBook Pro, Apple, Cupertino, CA, USA). There are four electrodes attached to the inner wall of the bathtub. The electrodes are hemispheres (stainless steel, Dragonmarts Co. Ltd, Hong Kong S.A.R. of China) with diameters of 25 mm and placed on both sides at the same level as limbs. The electrodes are connected to the ECG monitoring device with shielded cables.

OpenBCI Ganglion Board is the biosensing hardware for providing imaging and recording of EMG, ECG, and EEG signals. The board communicated wirelessly to a computer via BLE. The board's sample rate is limited by the BLE bandwidth. BLE radio rate is limited to 200 Hz. Therefore, data were sampled at 200 Hz on each of the four channels and recorded on a computer. ECG signals were collected during subjects' bathing in a relaxed position as shown in Figure 24. In previous studies, the impact of different water temperatures on HRV during bathing was proved. With the increase in water temperature, some HRV features were different degrees of impact such as reduction or rising [93,102,103]. In Japan, the water temperature almost is between 38℃ and 42℃ during bathing [104]. Some subjects can't complete taking a bathing at a water temperature of 42℃ during rehearsal. Therefore, each subject completed five BTs at different water temperatures, 37 ± 0.5℃, 38 ± 0.5℃, 39 ± 0.5℃, 40 ± 0.5℃, and 41 ± 0.5℃. The initial water temperature was set before data collection. After the subjects entered the bathtub, a thermal insulation film was covered on the bathtub to reduce the loss of water temperature during bathing. The duration of each BT was controlled to 15 min. The lead II ECG signals were collected and used in this study.

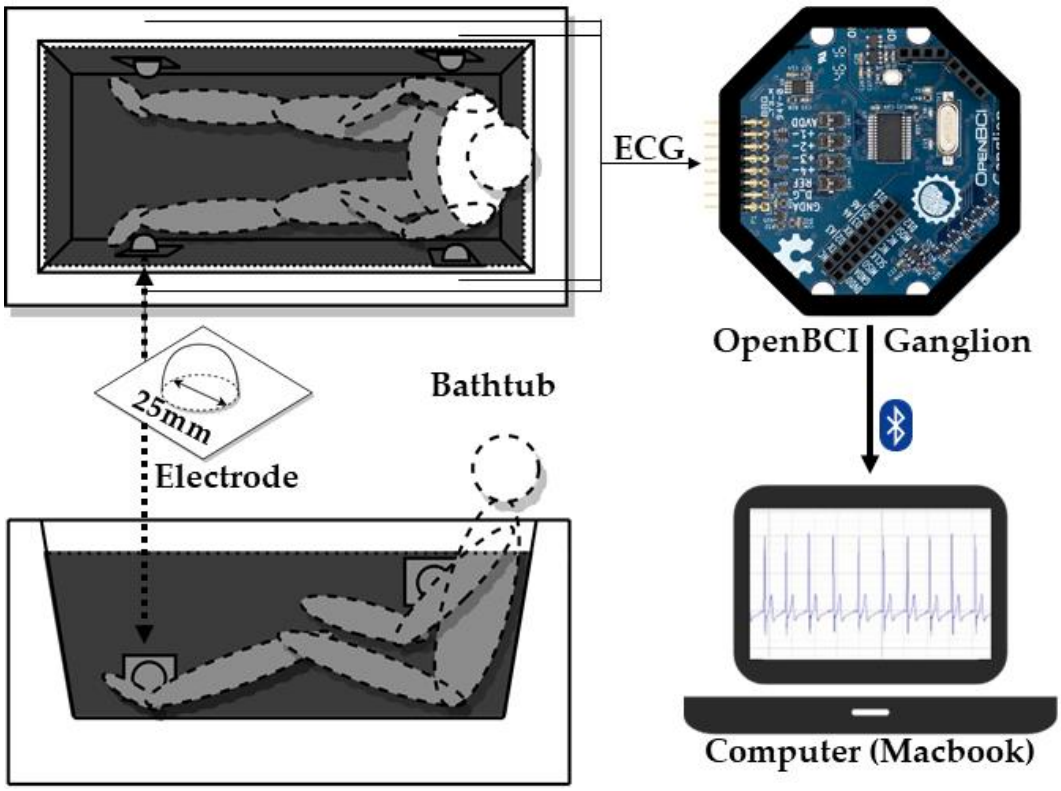

Figure 24. Scheme of the bathtub ECG monitoring system for BT

4.1.2. Exercise Stress Test

To collect the EST data, a treadmill ECG monitoring system was used. A schematic image is shown in Figure 25. This system consists of two components: an ECG monitoring device (BIOPAC MP36, BIOPAC Systems, Inc., Goleta, CA, USA) and a computer (Think-Pad X1 Carbon 7th, Lenovo, Hong Kong S.A.R. of

China). The exercise-induced stressor was an exercise on a treadmill (MATRIX T5x, Johnson Health Tech Japan Co. Ltd, Minatoku, Tokyo, Japan). Three adhesion-type electrodes (BlueSensor SP-00-S, Ambu A/S, Ballerup, Denmark) were attached to the subject's right chest, left subcostal, and right subcostal during data collection as shown in Figure 25. The electrodes were connected to the ECG monitoring device. The ECG monitoring device sampled the ECG signal at 1 kHz on one channel during the EST.

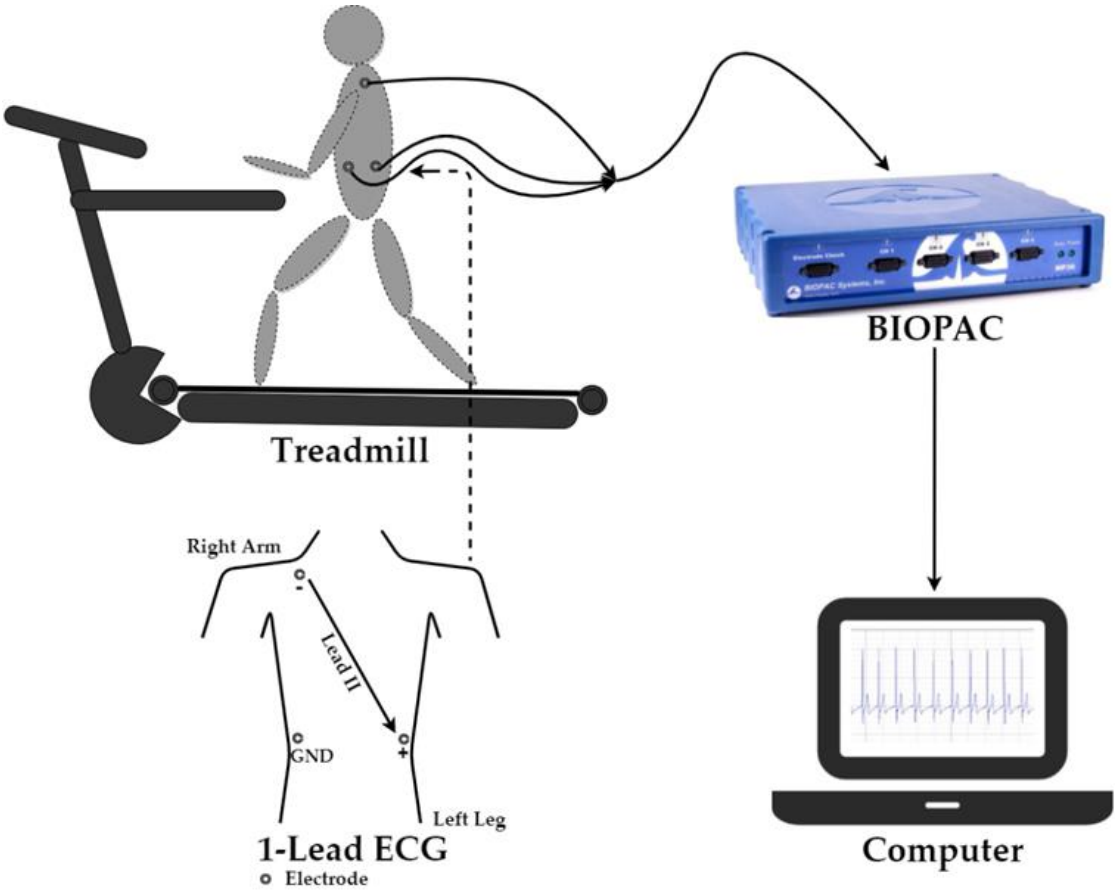

Figure 25. Scheme of the treadmill ECG monitoring system for EST

Data collection of the EST included the resting stage (R1) before the EST, the EST, the recovery stage (R2), and the relax stage (R3) after the EST. Data collection started at R1 and completed at R3. The EST was terminated before completion at the request of the subject or poor signs, e.g., fatigue, shortness of breath, wheezing, claudication, leg cramps, chest pain, being observed.

The modified Bruce protocol was used in this EST. As one of the most popular protocols utilized in exercise laboratories, the Bruce protocol has also been considered before data collection of the EST. Because of the heavy workload of the Bruce protocol for subjects as illustrated in Table 5, no subject completed it in its entirety during rehearsal. Therefore, the modified Bruce protocol that was utilized had a lower workload than the standard test as illustrated in Table 5 [89]. In R1, R2, R3, and the EST, the duration of each stage was 3 min, and the total duration of data collection was 30 min. Each subject completed data collection of the EST twice. The lead II ECG signals were collected for processing and analysis in this study.

Table 5. Bruce protocol and modified Bruce protocol for EST.

		Bruce Protocol		Modified Bruce Protocol	
Stage	**Duration (min)**	**Speed (km/h)**	**Grade (%)**	**Speed (km/h)**	**Grade (%)**
1	3	2.7	10	2.7	0
2	3	4.0	12	2.7	5
3	3	5.5	14	2.7	10
4	3	6.8	16	4.0	12
5	3	8.0	18	5.5	14
6	3	8.9	20	6.8	16
7	3	9.7	22	8.0	18

4.2 Data Preprocessing

All the signal processing procedures were implemented using MATLAB (R2020b, The MathWorks, Inc., Natick, MA, USA). The ECG signals were collected using different devices at different sampling rates. The ECG signals of the EST were sampled using BI-OPAC MP36 at 1 kHz. The ECG signals of the BT were sampled using OpenBCI Ganglion at 200 Hz and were upsampled from 200 Hz to 1 kHz for compromising with the former.

First, the ECG signals of the BT and EST were decomposed into seven levels by multilevel one-dimensional wavelet decomposition using one of Daubechies wavelets, “db8,” the final approximation coefficient was taken as the baseline drift and subtracted from the original signal. Second, a Butterworth bandpass filter was implemented to remove powerline noise and HF distortions. Then, R wave peaks detection was implemented after noise removal. The RRI is defined as the sequence of the time intervals occurring between each pair of consecutive R wave peaks. The RRIs were calculated based on the ECG signal R wave peaks detected. Finally, the NNI was calculated based on the RRI where unreliable RRI were excluded. The NNI dataset of the EST was calculated based on 3 min ECG signals of each stage. The NNI dataset of the BT was calculated based on each 30 s segmentation ECG signal. Figure 26 shows an example of fully BT and EST ECG signal preprocessing in 10 s, including signal detrending, signal denoising, and R wave peaks detection. In Figure 26, (a) shows the signal processing of a BT ECG and (b) shows the signal processing of an EST ECG signal. The 10 s BT and EST ECG signals are extracted from the ECG signals of subject V’s BT and EST. The collection condition of BT ECG signals is at the water temperature of 39 ℃. The EST ECG signals are 10 s of stage 5 of test I.

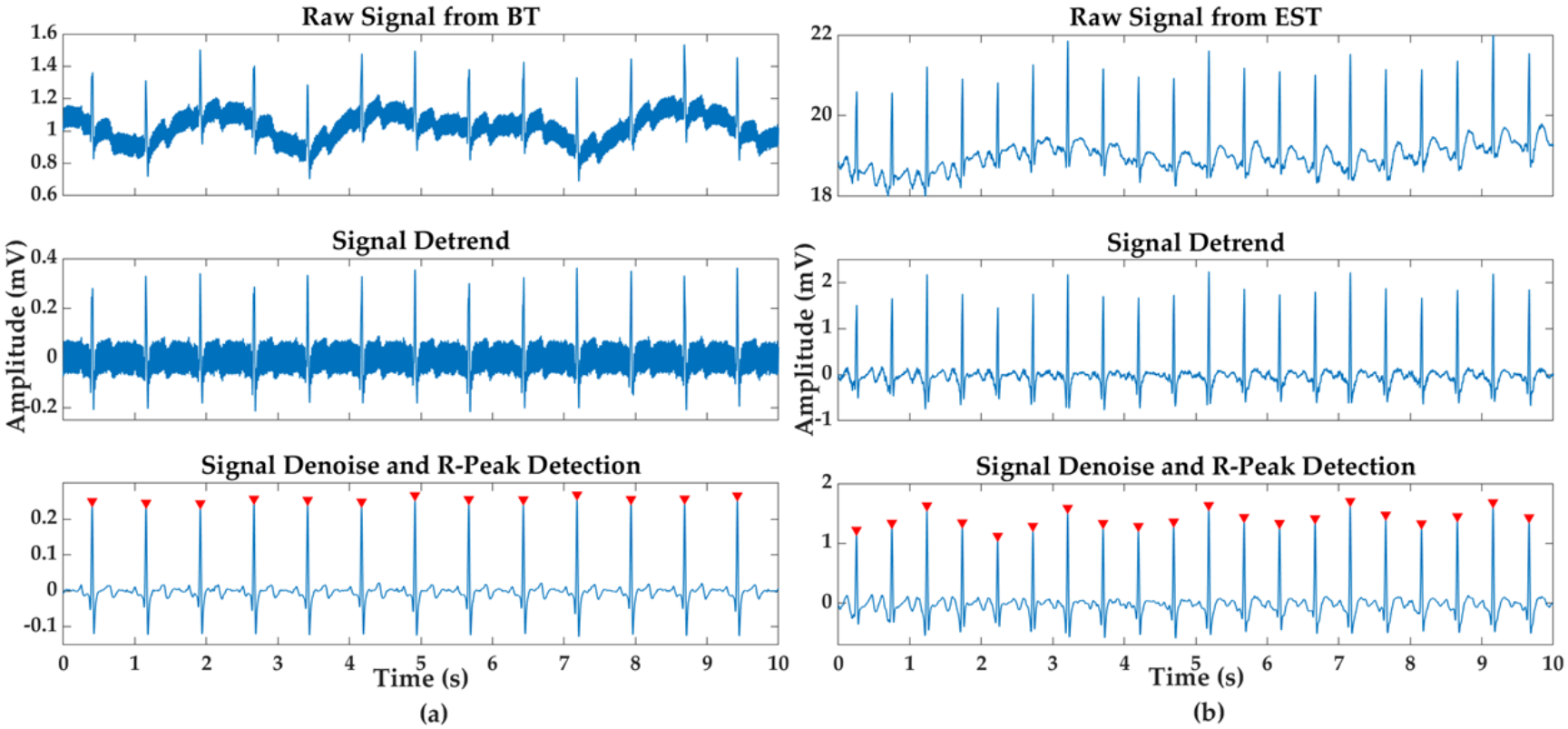

Figure 26. An example of ECG signal preprocessing and R-peak detection in 10 s. (a) BT ECG signal, (b) EST ECG signal.

4.3 HRV Feature Extraction

In this study, the obtained NNI data after signal preprocessing including denoising and R wave peak detection were used to extract HRV features. To reflect the heart functionalities comprehensively during the EST and BT, HRV features were extracted in the time domain, frequency domain, and nonlinear domain. All extracted HRV features are common features in use. In the nonlinear domain, features alpha 1 and alpha 2 of detrended fluctuation analysis (DFA) describe short-term and long-term fluctuation, respectively. Therefore, DFA alpha 1 was extracted. The extracted HRV features are summarized in Table 6 [34,46,105].

Table 6. Selected HRV features in the time domain, frequency domain, and nonlinear domain.

	Time Domain	Frequency Domain	Nonlinear
HRV Feature	NNmax	Total power	SD1
	NNmin	VLF	SD2
	NNmean	LF	DFA alpha1
	NNmedian	HF	
	SDNN	LF norm	
	NN50	HF norm	
	pNN50	LF peak	
	RMSSD	HF peak	
	HRmean	LF/HF	
	SDHR		
	HRV triangular index		

4.4 Principal Component Analysis

Twenty-three HRV features in the time domain, frequency domain, and nonlinear domain were extracted, some of which have strong correlations. The high-dimensionality limits exploration of the data, therefore, it is necessary to extract the important information from the 23 HRV features. PCA is a multivariate technique that analyzes the data and de-scribes several intercorrelated quantitative dependent variables. It is used to extract the important information from the data and represent the data as new variables called principal components. It has become one of the most useful tools for data modeling, compression, and visualization [105,106,107]. PCA was implemented for each of the 23 HRV features data of the BT, and all the sum of percentages of the first two principal components (PCs) are above 95% as shown in Figure 27.

Therefore, the first two PCs as the two main PCA components were used to approximate the 23 HRV features data. The 23 HRV features data of the BT were implemented in dimensionality reduction to two-dimensional (2-D) HRV data of the BT. The new 2-D HRV data of the EST were calculated using the PC coefficients of the BT HRV features data.

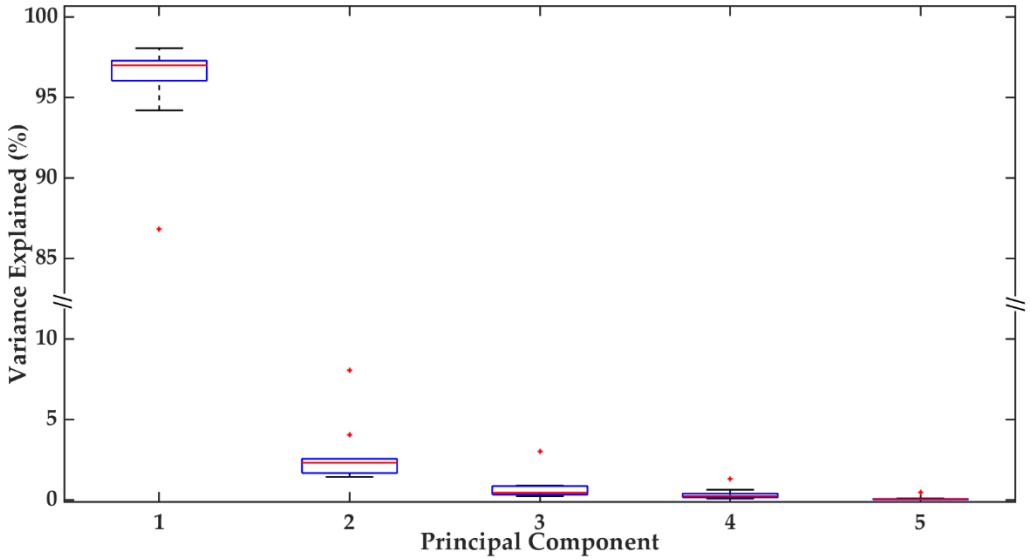

Figure 27. The first five PCs in PCA of BT HRV features

Therefore, the first two PCs as the two main PCA components were used to approximate the 23 HRV features data. The 23 HRV features data of the BT were implemented in dimensionality reduction to two-dimensional (2-D) HRV data of the BT. The new 2-D HRV data of the EST were calculated using the PC coefficients of the BT HRV features data.

4.5 Correlation Analysis of the Bathing Test and Exercise Stress Test

To explore the potential correlation between the BT and EST, the Voronoi diagram was used to cluster the BT data based on the Voronoi diagram generated from the EST da-ta. In the 2-D HRV data of the BT and EST after PCA, two main PCA components (PC1 and PC2) were selected. PC1 and PC2 of the EST were used to generate a 2-D Voronoi diagram of EST Stages 1–7. For the 2-D HRV data of each subject's two ESTs, the mean of PC1 and mean of PC2 of each stage were calculated to be the site point in the Voronoi diagram of each stage in the Voronoi diagram. PC1 is the abscissa value and PC2 is the ordinate value. The site point of each stage was used to generate a Voronoi region on the Voronoi diagram. As shown in Figure 28, St. 1–7 are the site points of Stages 1–7, and the seven Voronoi regions correspond to the seven stages of the EST. The 2-D HRV data after PCA of 30 s duration before and after per minute during the BT are calculated as the mean of the data for the corresponding duration. In each duration of the BT, the mean of PC1 and mean of PC2 are the feature point's abscissa value and ordinate value, respectively. To evaluate the equivalent EST stage of each duration of the BT, the EST site point closest to the BT feature points was queried. The HRV behaviors of the EST stage correspond to the closest site point and this BT feature point has the highest similarities. The EST stage corresponding to the closest site point serves as the equivalent EST stage

of this BT feature point. Euclidean distance is used to query the EST site point closest to the BT feature points. The Euclidean distance can be calculated using the following equation:

$$D = \sqrt{(X_{BT} - X_{EST})^2 + (Y_{BT} - Y_{EST})^2}$$

where X_{BT} is the abscissa value of the BT feature point, Y_{BT} is the ordinate value of the BT feature point, X_{EST} is the abscissa value of the EST site point, Y_{EST} is the ordinate value of the EST site point, and D is the Euclidean distance between the BT feature point and EST site point. The EST site point with the smallest distance from the BT feature point is the site point with the most similar feature. The EST stage represented by this site point is the stage to which the highest probability of the BT at the present bathing conditions represented by this feature point is equivalent. The equivalent EST stage in terms of HRV behaviors of the BT feature point was determined based on the corresponded EST stage of the closest EST site point.

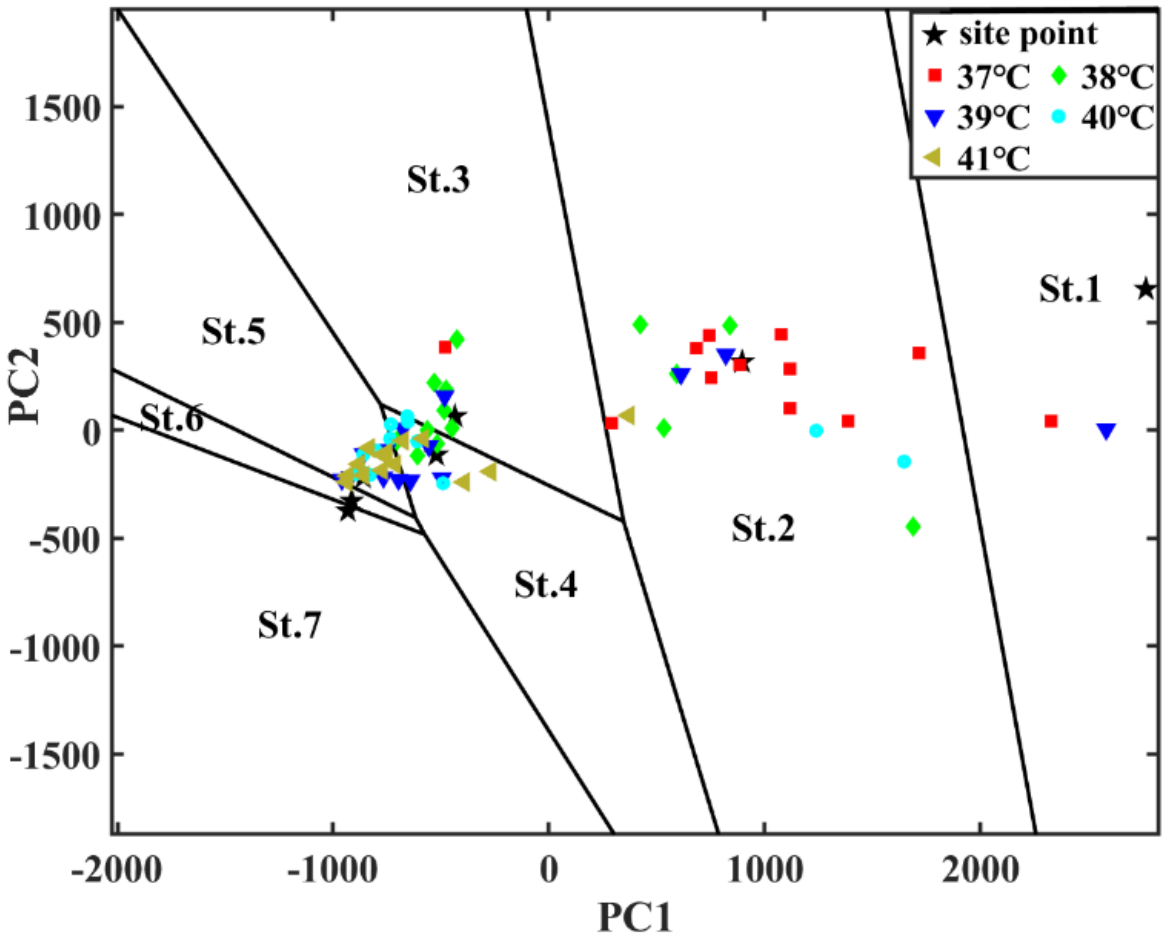

Figure 28. A distribution sample of the two main PCA components in the HRV of the BT at five water temperatures on a Voronoi diagram generated by EST Stages 1–7 (subject V)

As shown in Figure 28, the BT feature points of 37℃ water temperature are mostly located in the Voronoi region of Stage 2. The BT feature points of 38℃ water temperature are mostly located in the Voronoi region of Stages 3 and 4. The BT feature points of 39, 40, and 41℃ water temperature are mostly located in the Voronoi region of Stages 4 and 5.

To explain the similarity of HRV behaviors between the BT and EST more clearly, the original seven EST stages are grouped into three exercise stages,

namely, low stage, medium stage, and high stage. Stages 1 and 2 in the EST are merged as the low stage. The medium stage consists of Stages 3 and 4 in the EST. The high stage contains Stages 5, 6, and 7 in the EST. The mean of Stages 1 and 2 of two ESTs is used as the site point for the low stage. The site point of the medium stage is generated by the mean of Stages 3 and 4. The mean of Stages 5, 6, and 7 of two ESTs is used as the site point for the high stage. A 2-D Voronoi diagram of the three regions for the low, medium, and high stages was generated using the same method. The regions where the BT feature points are located are confirmed in the Voronoi diagram with the same method. As shown in Figure 29, for BTs at the five water temperatures of one subject, the BT feature points are located on a 2-D Voronoi diagram. The Voronoi diagram is generated and three Voronoi regions are generated by the site points of low, medium, and high stages.

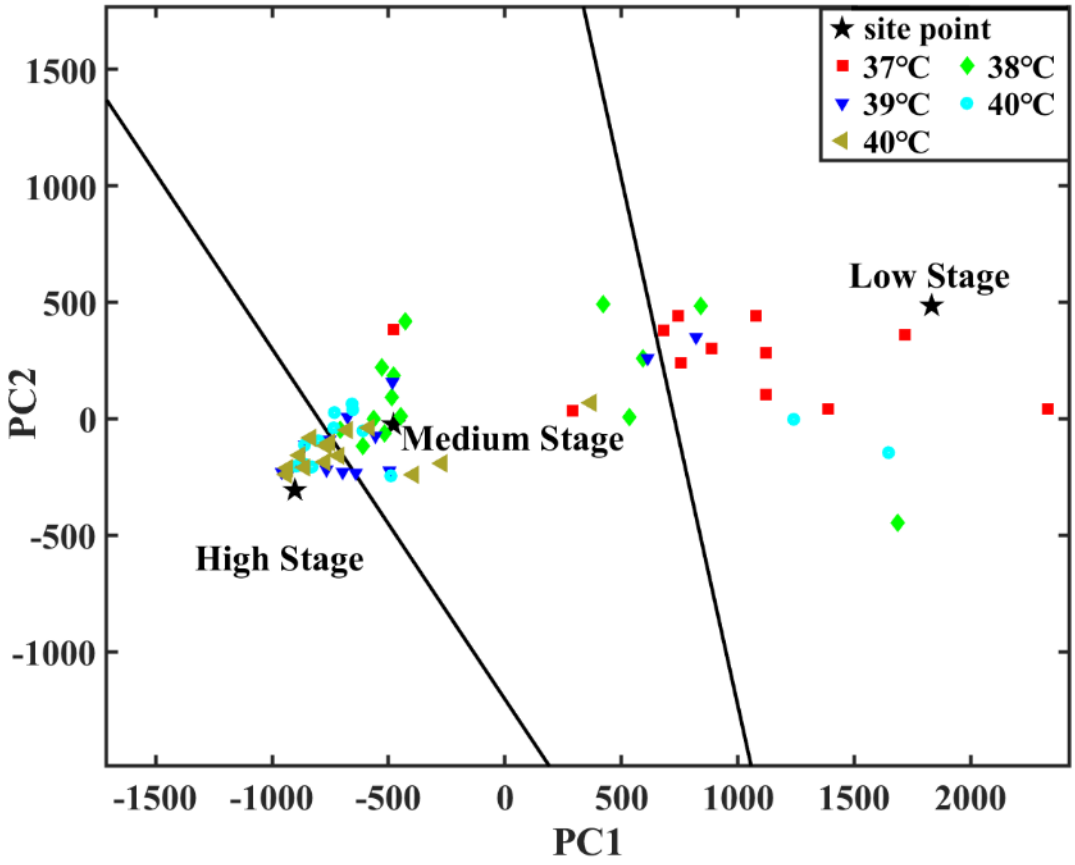

Figure 29. A distribution sample of the two main PCA components in the HRV of the BT at the five water temperatures on a Voronoi diagram generated by low, medium, and high stages (subject V)

For all subjects, the equivalent EST stages of BTs at the five water temperatures were calculated. The means of the corresponding stage of all subjects under the same water temperature and bathing duration during the BT were calculated. With water temperature as the x-axis, bathing duration as the y-axis, corresponding stage as the z-axis, the fitting surface was implemented using cubic spline interpolation and polynomials.

4.6 Results

4.6.1. Biometric Information of Subjects and Completion Status of Data Collection

All the biometric information of subjects was obtained, and the completion status of the EST and BT is illustrated in Table 7. Fifty BTs were implemented completely, and the end-stages in 7 of 20 ESTs are Stage 7. Three subjects reached Stage 7 at the end-stage in tests I and II. According to the experiment diary, subjects who completed Stage 7 exercise frequently. To avoid chance, ensure more accurate results and reduce errors, two ESTs were implemented. As illustrated in Table 7, the number values of tests I and II indicate the reached end-stage. Decimals indicate the test of the stage is started but not fully implemented. 3, 5, and 7 after the decimal point represent 1 min, 1.5 min, and 2min respectively. For example, 5.3 indicates Stage 5 is completed and Stage 6 is completed for 1 min; 6.5 represents Stage 6 is completed and Stage 7 is implemented for 1.5 min; 6.7 indicates Stage 6 is finished and Stage 7 is stopped at 2 min.

Table 7. Biometric information of subjects and test completion status.

Subject	Age (Years)	Body Weight (kg)	Height (cm)	Test Completion Status		
				Bathing (1–5)	Exercise Stage (1–7)	
					Test I	Test II
I	39	72	176	5	6.0	5.5 *
II	29	67	179		6.0	5.3 *
III	28	80	173		6.7 *	6.3 *
IV	28	71	176		6.5 *	5.3 *
V	26	69	172		7.0	7.0
VI	25	70	177		5.5 *	6.0
VII	24	75	173		6.0	5.5 *
VIII	29	69	184		6.5 *	7.0
IX	28	68	168		7.0	7.0
X	25	70	175		7.0	7.0

Note: all subjects were healthy males.

* Decimals indicate the test of the stage is started but not fully implemented. 6.7 indicates Stage 6 is completed and Stage 7 is implemented for 2 min. 3 and 5 after the decimal point represent 1 min and 1.5 min, respectively.

4.6.2. Evaluation of the Relationship Between Bathing Conditions and EST Stages

EST stages are grouped into three stages (low, medium, and high) with a Voronoi diagram using the 2-D HRV data of the EST after PCA analysis of each subject. The EST stages with the highest probability corresponding to the BT conditions at different water temperatures and bathing durations were calculated. In all equivalent EST stages of the BTs, the low stage accounts for 17.86%, medium stage accounts for 52.86%, and high stage accounts for 29.29%. The means and standard deviations of water temperatures of equivalent low, medium, and high stages are 38.21 ± 1.28, 38.93 ± 1.38, and 39.61 ± 1.28℃, respectively. Of water temperatures corresponding to the low stage, 37℃ accounts for 40.80% and 38℃ accounts for 24.00%. Of water temperatures corresponding to the medium stage, 37, 38, 39, 40, and 41℃ account for 19.19%, 23.51%, 20.54%, 18.92%, and 17.84%, respectively. 39, 40, and 41℃ account for 21.84%, 25.73%, and 32.04%, respectively, of the water temperatures corresponding to the high stage in terms of HRV behaviors. The details of investigating the relationship between water temperature and the equivalent EST stage (Bruce and grouped) in terms of HRV behaviors are illustrated in Tables 8 and 9, respectively. As shown in Table 8, in the BT at 37℃ water temperature, the equivalent EST Bruce stages are mainly concentrated in Stages 2 (23.57%) and 3 (38.57%). In the BT at 38℃, the equivalent EST Bruce stages are mainly centralized in Stages 3 (36.43%) and

4 (27.14%). About the BT at 39℃, the equivalent EST Bruce stages are mainly distributed in Stages 3 (27.14%), 4 (33.57%), and 5 (21.43%). In the BT at 40℃, the equivalent EST Bruce stages are mainly centered in Stages 4 (35.71%) and 5 (20.71%). In the BT at 41℃, the equivalent EST Bruce stages are mainly distributed in Stages 4 (37.14%) and 5 (26.43%). As the water temperature increases from 37℃ to 41℃, the main distribution of equivalent EST Bruce stages is from stages 2 and 3 up to stages 4 and 5. The relationship between water temperature and the equivalent EST grouped stages is more obviously illustrated in Table 9. As the water temperature increased from 37℃ to 41℃, the proportion of the low stage of the equivalent EST grouped stage decreased from 36.43% to 5.71%, and the proportion of the high stage increased from 12.86% to 47.14%.

Table 8. Relationship between water temperature and the equivalent EST Bruce stage.

Stage	Water Temperature (°C) Count (%)				
	37	38	39	40	41
1	23 (16.43)	13 (9.29)	12 (8.57)	5 (3.57)	5 (3.57)
2	33 (23.57)	18 (12.86)	9 (6.43)	16 (11.43)	5 (3.57)
3	54 (38.57)	51 (36.43)	38 (27.14)	26 (18.57)	27 (19.29)
4	17 (12.14)	38 (27.14)	47 (33.57)	50 (35.71)	52 (37.14)
5	13 (9.29)	9 (6.43)	30 (21.43)	29 (20.71)	37 (26.43)
6	0 (0)	2 (1.43)	4 (2.86)	3 (2.14)	1 (0.71)
7	0 (0)	9 (6.43)	0 (0)	11 (7.86)	13 (9.29)

Table 9. Relationship between water temperature and the equivalent EST grouped stage.

Stage	Water Temperature (°C) Count (%)				
	37	38	39	40	41
Low	51 (36.43)	30 (21.43)	19 (13.57)	17 (12.14)	8 (5.71)
Medium	71 (50.71)	87 (62.14)	76 (54.29)	70 (50.00)	66 (47.14)
High	18 (12.86)	23 (16.43)	45 (32.14)	53 (37.86)	66 (47.14)

The means of the corresponding stage of all subjects under the same water temperature and bathing duration during the BT were calculated. The 3-D relationship diagram between water temperature, bathing duration, and EST stage is shown in Figure 30. Cubic splines were used to interpolate in Figure 30.

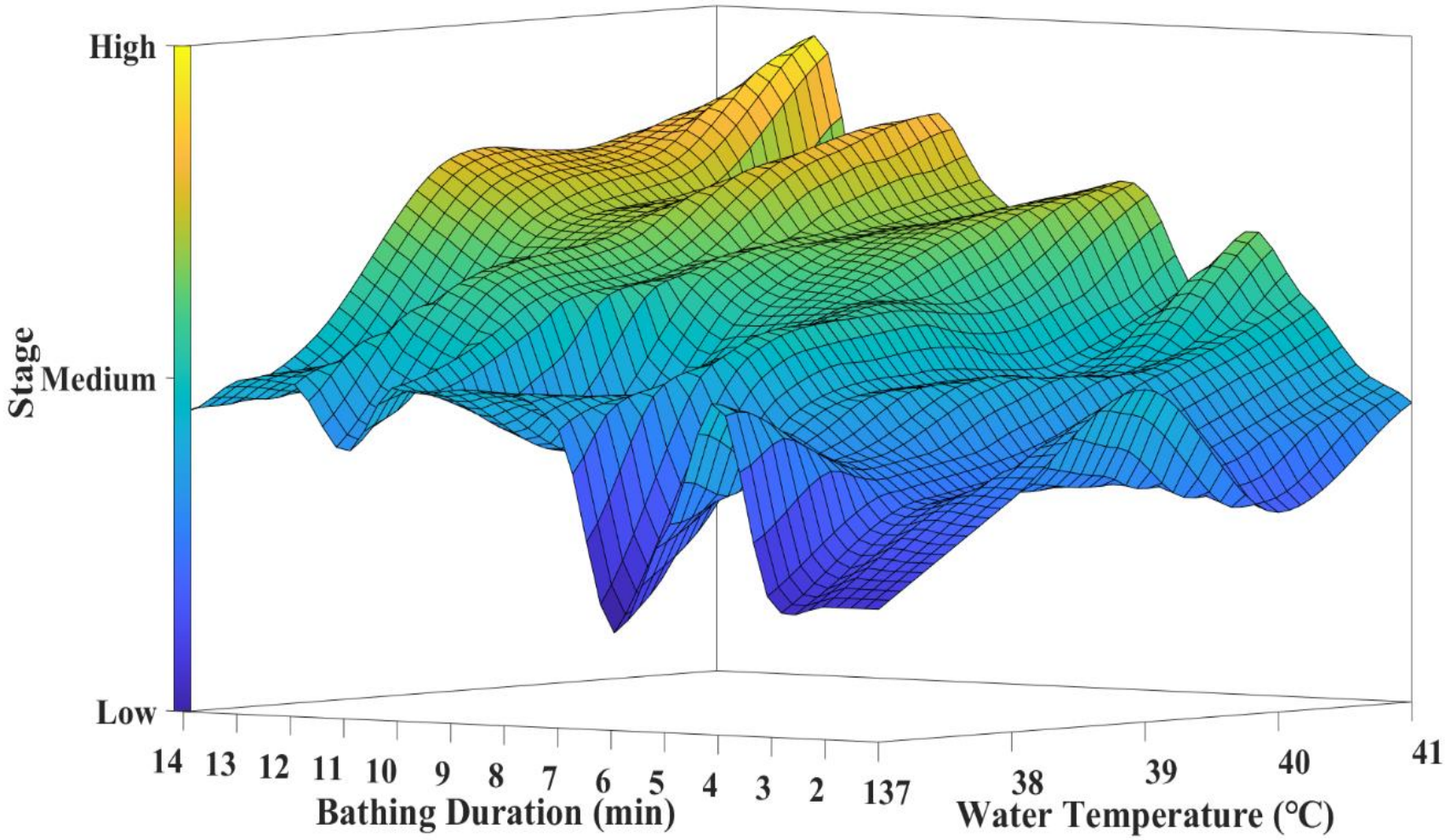

Figure 30. Relationship surface between water temperature, bathing duration, and the equivalent EST stage in terms of HRV behaviors

To show the relationship more intuitively between water temperature, bathing duration, and equivalent EST stage, surface fitting was implemented using polynomials. Figure 31 shows the relationship surfaces fitted by the 1st-order (a), 2nd-order (b), 3rd-order (c), and 4th-order (d) polynomial surfaces. At the water temperature of 41℃, the equivalent EST stage after 14 min of bathing is the highest. As the water temperature and bathing duration increase, so does the equivalent stage in terms of HRV behaviors.

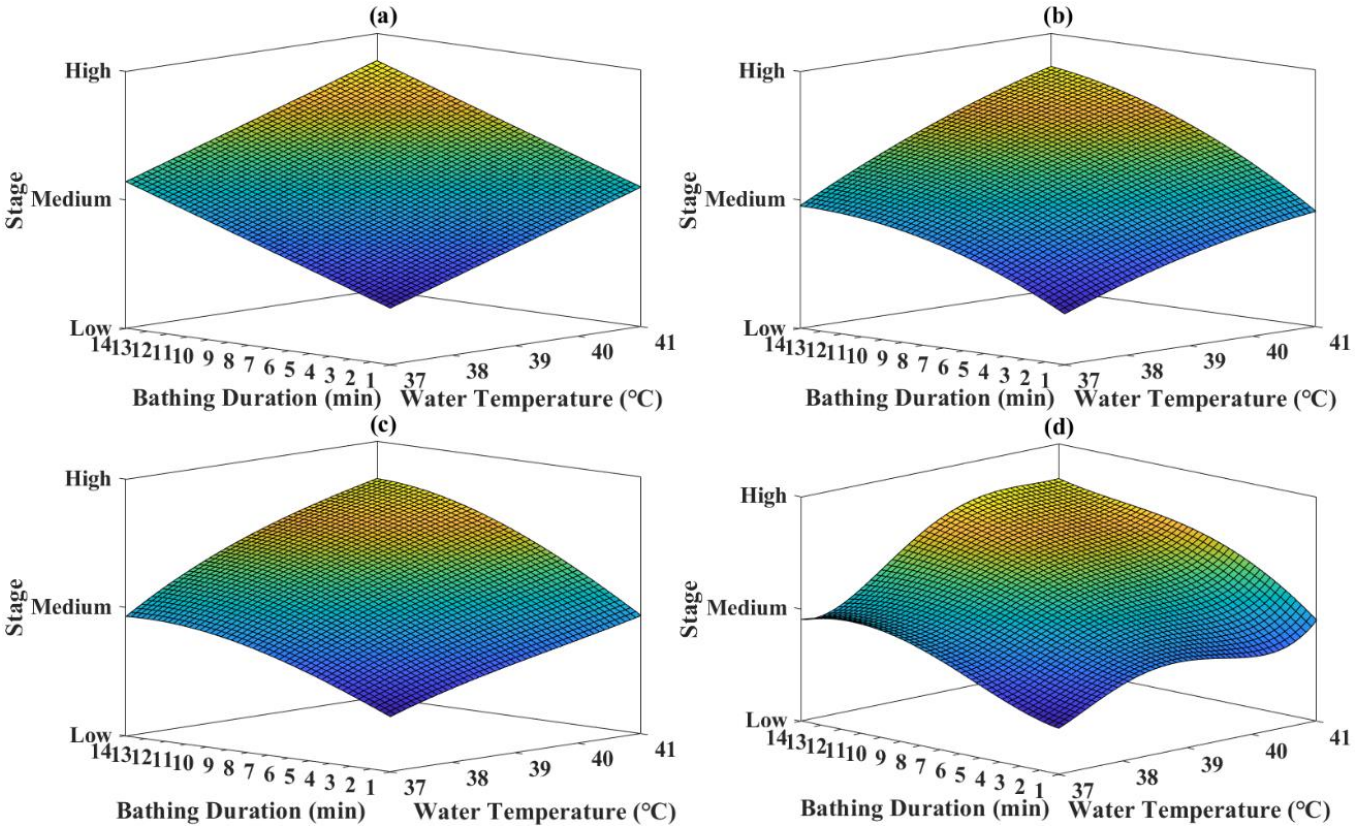

Figure 31. Relationship surfaces using polynomial fitting. (a) to (d), 1st- to 4th-order polynomials, respectively, are implemented.

The approximation formulas of 1st- to 4th-order polynomials are as follows:

$$ST = -4.558 + 0.1607 \times WT + 0.05389 \times BD \quad (1)$$

$$ST = -27.1 + 1.353 \times WT - 0.112 \times BT - 0.01582 \times WT^2 + 0.005516 \times WT \times BD - 0.003283 \times BD^2 \quad (2)$$

$$\begin{aligned} ST = {} & -185.6 + 14.03 \times WT - 2.533 \times BD - 0.3526 \times WT^2 + 0.1267 \times WT \times BD \\ & + 0.005415 \times BD^2 + 0.002976 \times WT^3 - 0.001523 \times WT^2 \times BD \\ & - 0.000158 \times WT \times BD^2 - 0.0001128 \times BD^3 \end{aligned} \quad (3)$$

$$\begin{aligned} ST = {} & 41910 - 4375 \times WT + 343 \times BD + 171.1 \times WT^2 - 26.2 \times WT \times BD - 0.7042 \times BD^2 \\ & - 2.973 \times WT^3 + 0.6657 \times WT^2 \times BD + 0.04253 \times WT \times BD^2 - 0.011 \times BD^3 \\ & + 0.01935 \times WT\text{^}4 - 0.005623 \times WT\text{^}3 \times BD - 0.000623 \times WT\text{^}2 \times BD\text{^}2 \\ & + 0.00002624 \times WT \times BD^3 + 0.00002185 \times BD^4 \end{aligned} \quad (4)$$

where WT is the water temperature of the BT, BD is the bathing duration of the BT, and ST is the equivalent EST stage.

Formulas (1) to (4) are approximation formulas of 1st- to 4th-order polynomials of the relationship fitting surface (a) to (d) in Figure 31, respectively. Formula (1) is bivariate 1st- order polynomials and the relationship fitting surface is a flat. Water temperature and bathing duration are proportional to the equivalent EST grouped stage. Formulas (2) and (3) are bivariate 2nd- and 3rd-order polynomials and the relationship fitting surfaces (b) and (c) are more radian than (a). Formula (4) is bivariate 4th- order polynomials and the trend of

relationship fitting surface (d) is the closest to Figure 30 in Figure 31 (a)- (d). The goodness of fit is illustrated in Table 10. The sum of squares due to error (SSE) of the fitting values and the original value is calculated to show the dispersion of the fitting values and the original value. The formula is as follow:

$$SSE = \sum_{m=1}^{M} \left(ST_m - \widehat{ST}_m\right)^2$$

where ST_m and $\widehat{ST}_m$ represent the original and fitted values of the equivalent EST grouped stage at the same water temperature and bathing duration, respectively, and M is the number of sets of samples. The closer SSE is to 0, the better the fitting effect. The coefficient of determination (R^2) is calculated to evaluate the fitting effect of the fitting function. When the R^2 result is between 0 and 1 and the closer the result is to 1, the better the fitting effect is. The formula is as follow:

$$R^2 = 1 - \frac{\sum_m^M \left(ST_m - \widehat{ST}_m\right)^2}{\sum_m^M (ST_m - \overline{ST}_m)^2}$$

As illustrated in Table 10, comparing the SSE and R^2 results of 1st- to 4th-order polynomials, SSE of 4th-order polynomials is the closest to 0, and R^2 is the closest to 1.

Table 10. SSE and R^2 of 1st- to 4th-order polynomials.

Order	SSE	R^2
1	1.646	0.8078
2	1.371	0.8274
3	1.359	0.8414
4	1.171	0.8633

4.7 Summary

In this study, we collected 10 subjects' ECG signals during the BT and EST, and explored if daily bathing can serve as a potential alternative means of EST based on HRV behaviors evaluated in three analysis domains. Stressful loads by different water temperatures and bathing durations of the BT correspond to different exercise stages in terms of HRV behaviors. As shown in Figure 31, in general, the higher water temperatures during bathing and longer bathing durations, the higher the equivalent stages. More specifically, in the high stage (Stages 5–7), 32.04% equivalent stages in terms of HRV behaviors correspond to bathing at 41°C water temperatures and 25.73% correspond to bathing at 40°C. In all equivalent EST stages of BTs, the medium stage accounts for 52.86%. Therefore, bathing can be an alternative to light EST in daily life.

In our previous study, we defined an SI to quantify the stress level [62]. The SI mainly explains psychological stress and is not applicable to this study. In this study, a new procedure is explored for an alternative to EST. HRV features were extracted to reflect the heart behavior during the EST and BT. Different levels of load are generated by bathing with different water temperatures and bathing durations. Different bathing loads correspond to different exercise stages in terms of HRV behaviors as shown in Figure 31. In all equivalent EST stages of BTs, the medium stage accounts for 52.86%. The equivalent EST stages in terms of HRV behaviors of BTs are mostly distributed in the low and medium stages. It is hard to correspond Stage 7 to the BT with normal and nonextreme conditions. If a certain equivalent EST stage is needed to implement during daily health monitoring, it is needed to take bathing at the corresponding water temperature for the corresponding bathing duration.

The EST is a routine procedure in the clinic to evaluate cardiovascular functions but is commonly too demanding and sometimes risky for some subjects [87,88]. As illustrated in Table 7, even with the modified Bruce protocol during ESTs, we confirmed that most sub-jects did not complete Stage 7 in the end-stage. In addition, there are some contraindications to the EST, acute myocardial infarction within 2 days, ongoing unstable angina, active endocarditis, decompensated heart failure, acute myocarditis or pericarditis, etc. [81]. In Japan, bathing is popular with many people and has become a daily activity [60]. Bathing may not only be safe for patients with heart failure but may even briefly improve hemodynamics with a short bathing duration [108]. It was confirmed that warm

bathing, sauna bathing, and spring bathing improve cardiac function and have beneficial effects with heart failure patients [109,110,111,112]. Lee et al. proved that forest bathing has positive effects on physical and mental health [113]. Bathing not only can correspond to a light stress stage but also benefits cardiovascular function and physical and mental health. The BT is safer, more comfortable, and more convenient.

In this study, the relationship between water temperature, bathing duration, and EST grouped stages was investigated. A detailed analysis of the relationship with Stages 1–7 of the modified Bruce protocol was not implemented. Due to the amount of data, complex classification methods are not used. All subjects were male students. There is great individual variability among subjects. Data collection is in progress. Future work will involve more data from different age and gender groups. Grouping subjects for more precise results. More methods will be explored to reveal more outcomes.

This study revealed the relationship between BT and EST by investigating the HRV behaviors in two tests. As the water temperature and bathing duration increase during bathing, the equivalent EST stages also increase. The equivalent EST grouped stages are mainly concentrated in the medium stage (52.86%). An alternative procedure to light EST for daily life is provided. In the BT, the water temperature and bathing duration can be chosen to implement the corresponding exercise stage. This can serve as a tool for daily monitoring of the health condition or as a reference for clinical application.

Chapter 5

Conclusion and Future Research

In addition to the role of daily cleaning, bathing can also be used as a means of daily healthcare monitoring. In this dissertation, the bathtub ECG monitoring system is optimized. The most suitable electrode for bathtub ECG collection during bathing is selected based on the evaluation of the ECG signal quality. Using heart rate variability analysis to estimate the optimal bathing time, combined with the stress index, the effect of stress on the optimal bathing time is obtained. Stress has an obvious effect on optimal bathing time. Stress delays the optimal bathing time. On the other hand, in high-stress situations, it takes longer to achieve the comfort of bathing. Bathtub ECG as a potential alternative to light stress test in daily life is proposed. The correlation between bathing and exercise stress test is explored. The relationship between bathing duration, water temperature, and the exercise stress test stage is analyzed. Twenty-three HRV features are used to group different bathing conditions corresponding to the EST stages using the Voronoi diagram method in terms of HRV behaviors. In all equivalent EST stages of bathing tests at the five water temperatures, the low stage, medium stage, and high stage account for 17.86%, 52.86%, and 29.29%, respectively. The higher water temperatures and longer bathing durations in bathing test correspond to higher

stages in the EST. The BT at the most severe condition of 41 °C and 15 min corresponds to a high EST stage in terms of HRV behavior. Daily bathing can serve not only for cleaning and healthcare monitoring but also as a reference for an at-home alternative to the EST.

The study on the effect of stress on bathing includes only one subject, and although the experiment is followed for a long time, the sample is single, and differences between different subjects could not be found. If there is an opportunity to continue this study in the future, it is hoped that the number of subjects can be increased. Comparing whether the optimal bathing time is the same for different subjects under stress.

There is still room for improvement in this bathtub ECG monitoring system. During ECG signal collection with the bathtub ECG monitoring system, only three channels are used. However, the OpenBCI Cyton + Daisy board supports a maximum of 16 channels to collect data simultaneously. The future research direction is the development of a multi-lead bathtub ECG monitoring system. The number of leads can be expanded to 12 leads. Back lead ECGs can also be acquired. Collecting ECG signals from more angles can monitor the health of the heart more comprehensively.

In the study on bathtub ECG as a potential alternative to light stress test in daily life, there are ten subjects who participated. There are differences between each subject. But some common features can still be found. The relationship surfaces of subjects who exercise regularly are similar. In the future study,

increasing the number of subjects is inevitable. At the same time, subjects of different genders, different ages, and different regions should be added. With enough data, other methods can be tried to refine the study. More interesting outcomes can be found.

There are many interesting findings in the study of the bathtub ECG. These interesting ideas can be carried out in future research. For example, in the ECG signal during bathing, the component of baseline drift is similar to the respiratory signal. Trying to extract the respiratory signal in the bathing ECG. In addition to the duration of bathing and water temperature, there are other bathing environment variables, such as bathing agents and sounds. Trying to explore the setting of the optimal bathing environment. There are also some studies on bathing safety that can be carried out, such as fall monitoring and drowning monitoring. Trying different signals such as wifi signals to monitor in the bathroom.

Acknowledgment

I sincerely acknowledge my supervisor Prof. CHEN Wenxi for his continuous advice, guidance, support, and help both in study and in life during my master's and doctoral program.

I would like to sincerely thank my dissertation review members, Prof. Cohen, Prof. Hisada, and Prof. Yen, for their review and constructive comments.

I appreciate so much my parents and sister for supporting me both spiritually and materially. Thank you very much for your silent support and understanding.

I sincerely thank Mrs. HUANG, Prof. CHEN's wife, for the care over the past five years.

I am grateful to Ms. MASHIKO Rika and the staff of university who provided lots of help.

My heartfelt thanks to the people who have helped me during this pandemic.

I sincerely thank the owner of Saikarou Chinese restaurant for giving me a part-time job when I was in financial trouble.

I would like to express my sincere thanks to Rotary Yoneyama Memorial Foundation and Aizu-Wakamatsu West Rotary Club for supporting me.

Thank you, Dr. ZHOU, for the light in the darkness.

References

[1] Richard, L.; Hurst, T.; Lee, J. Lifetime exposure to abuse, current stressors, and health in federally qualified health center patients. J. Hum. Behav. Soc. Environ. 2019, 29, 593–607.

[2] Everly, G.S.; Lating, J.M. The anatomy and physiology of the human stress response. In A Clinical Guide to the Treatment of the Human Stress Response. Springer. New York, NY, 2019, 19–56.

[3] Hemmingsson, E. Early childhood obesity risk factors: Socioeconomic adversity, family dysfunction, offspring distress, and junk food self-medication. Curr. Obes. Rep. 2018, 7, 204–209.

[4] Chrousos, G. Stress and disorders of the stress system. Nat Rev Endocrinol. 2009, 5, 374–381.

[5] McEwen, B.S.; Stellar, E. Stress and the Individual: Mechanisms Leading to Disease. Arch Intern Med. 1993, 153, 2093–2101.

[6] Kivimäki, M.; Steptoe, A. Effects of stress on the development and progression of cardiovascular disease. Nat. Rev. Cardiol. 2018, 15, 215.

[7] Mariotti, A. The effects of chronic stress on health: New insights into the molecular mechanisms of brain—Body communication. Futur. Sci. OA 2015,

1, FSO23.

[8] Tamashiro, K.L.; Sakai, R.R.; Shively, C.A.; Karatsoreos, I.N.; Reagan, L.P. Chronic stress, metabolism, and metabolic syndrome. Stress 2011, 14, 468–474.

[9] O'Connor, D.B.; Thayer, J.F.; Vedhara, K. Stress and health: A review of psychobiological processes. Annual review of psychology 2021, 74, 663–688.

[10] World Health Organization. OthersWorld Health Statistics Data Visualizations Dashboard. In Obtenido de World Health Statistics Data Visualizations Dashboard; WHO: Geneva, Switzerland, 2018; pp. 3–4. Available online: http//apps.who.int/gho/data/node. sdg (accessed on 20 February 2021).

[11] Aguiló, J.; Ferrer-Salvans, P.; Garc0ia-Rozo, A.; Armario, A.; Corb0i, Á.; Cambra, F.J.; Bailón, R.; González-Marcos, A.; Caja, G.; Aguiló, S.; López-Antón, R.; Arza-Valdés, A.; Garzón-ReyProject, J.M. ES3: Attempting to quantify and measure the level of stress. Rev. Neurol. 2015, 61, 405–415.

[12] McEwen, B.S.; Gianaros, P.J. Stress and allostasis-induced brain plasticity. Annual Review of Medicine 2011, 62, 431–445.

[13] McEwen, B.S.; Morrison, J.H. The brain on stress: Vulnerability and plasticity of the prefrontal cortex over the life course. Neuron 2013, 79, 19–29.

[14] McEwen, B.S.; Nasca, C.; Gray, J.D. Stress effects on neuronal structure: Hippocampus, amygdala, and prefrontal cortex. Neuropsychopharmacology 2016, 41, 3–23.

[15] Brosschot, J.F.; Verkuil, B.; Thayer, J.F. Generalized unsafety theory of stress: Unsafe environments and conditions, and the default stress response. International Journal of Environmental Research and Public Health 2018, 15, 464.

[16] Jarczok, M.N.; Jarczok, M.; Thayer, J.F. Work stress and autonomic nervous system activity. Handbook of Socioeconomic Determinants of Occupational Health: From Macro-level to Micro-level Evidence 2020, 1–33.

[17] Thayer, J.F.; Åhs, F.; Fredrikson, M.; Sollers, J.J.III; Wager, T.D. A meta-analysis of heart rate variability and neuroimaging studies: Implications for heart rate variability as a marker of stress and health. Neuroscience & Biobehavioral Reviews 2012, 36, 747–756.

[18]Wikipedia,Electrocardiography.Available online: https://en.wikipedia.org/wiki/Electrocardiography#cite note-FOOTNOTELilly201680-7 (accessed on 29 May 2022).

[19] Lilly, L. S. Pathophysiology of Heart Disease: A Collaborative Project of Medical Students and Faculty. Lippincott Williams and Wilkins, 2016.

[20] Walraven, G. Basic arrhythmias. Pearson; 7 edition, 2011.

[21] Braunwald, E. Heart Disease: A Textbook of Cardiovascular Medicine. Philadelphia, W.B. Saunders Co, 1997.

[22] Luz, E.J.D.S.; Schwartz, W.R.; Cámara-Chávez, G.; Menotti, D. ECG-based heartbeat classification for arrhythmia detection: A survey. Computer methods and programs in biomedicine 2016, 127, 144–164.

[23] Acharya, U.R.; Fujita, H.; Oh, S.L.; Hagiwara, Y.; Tan, J.H.; Adam, M. Application of deep convolutional neural network for automated detection of myocardial infarction using ECG signals. Information Sciences 2017, 415, 190–198.

[24] Corrado, D.; Pelliccia, A.; Heidbuchel, H.; Sharma, S.; Link, M.; Basso, C.; Biffi, A.; Buja, G.; Delise, P.; Gussac, I.; Anastasakis, A.; Borjesson, M.; Bjørnstad, H.H.; Carrè, F.; Deligiannis, A.; Dugmore, D.; Fagard, R.; Hoogsteen, J.; Mellwig, K.P.; Panhuyzen-Goedkoop, N.; Solberg, E.; Vanhees, L.; Drezner, J.; Mark Estes, N.A.III; Iliceto, S.; Maron, B.J.; Peidro, R.; Schwartz, P.J.; Stein, R.; Thiene, G.; Zeppilli, P.; McKenna, W.J. Recommendations for interpretation of 12-lead electrocardiogram in the athlete. European heart journal 2010, 31, 243–259.

[25] Kwok, Y.; Kim, C.; Grady, D.; Segal, M.; Redberg, R. Meta-analysis of exercise testing to detect coronary artery disease in women. The American journal of cardiology 1999, 83, 660–666.

[26] Bruce, R.A.; Hornsten, T.R. Exercise stress testing in evaluation of patients with ischemic heart disease. Progress in cardiovascular diseases 1969, 11, 371–390.

[27] Penzel, T.; McNames, J.; De Chazal, P.; Raymond, B.; Murray, A.; Moody, G. Systematic comparison of different algorithms for apnoea detection based on electrocardiogram recordings. Medical and Biological Engineering and Computing 2002, 40, 402–407.

[28] Van Mieghem, C.; Sabbe, M.; Knockaert, D. The clinical value of the ECG in noncardiac conditions. Chest 2004, 125, 1561–1576.

[29] Wikipedia, Heart rate variability. Available online: https://en.wikipedia.org/wiki/Heart rate variability#cite ref-53 (accessed on 29 May 2022).

[30] Rajendra Acharya, U.; Paul Joseph, K.; Kannathal, N.; Lim C.M.; Suri, J.S. Heart rate variability: a review. Med. Bio. Eng. Comput. 2006, 44, 1031–1051.

[31] Saul, J.P. Beat-to-beat variations of heart rate reflect modulation of cardiac autonomic outflow. Physiology 1990, 32–37.

[32] Levy, M.N.; Schwartz, P.J. Vagal control of the heart: Experimental basis and clinical implications. Futura Publishing Company. 1994.

[33] Schwartz, P.J.; PRIORO, S.G. Sympathetic nervous system and cardiac arrythmias. Cardiac electrophysiology: from cell to bedside. Philadelphia: WB Saunders CO 1990, 330, 43.

[34] Malik, M. Heart rate variability: Standards of measurement, physiological interpretation, and clinical use: Task force of the European Society of Cardiology and the North American Society for Pacing and Electrophysiology. Circulation 1996, 93, 1043–1065.

[35] Akselrod, S.; Gordon, D.; Ubel, F.A.; Shannon, D.C.; Berger, A.; Cohen, R.J. Power spectrum analysis of heart rate fluctuation: a quantitative probe of beat-to-beat cardiovascular control. Science 1981, 213, 220–222.

[36] Berger, R.D.; Akselrod, S.; Gordon, D.; Cohen, R.J. An efficient algorithm for

spectral analysis of heart rate variability. IEEE Trans. Biomed. Eng. 1986, 9, 900–904.

[37] Kamath, M.V.; Fallen, E.L. Power spectral analysis of heart rate variability: a noninvasive signature of cardiac autonomic function. Crit Rev Biomed Eng, 1993, 21, 245–311.

[38] Marked, V. Correction of the heart rate variability signal for ectopics and missing beats. Heart rate variability. Futura Publ. 1995, 75-85.

[39] Kobayashi, M.; Musha, T. 1/f fluctuation of heartbeat period. IEEE transactions on Biomedical Engineering 1982, 6, 456–457.

[40] Pagani, M.; Lombardi, F.; Guzzetti, S.; Rimoldi, O.; Furlan, R.; Pizzinelli, P.; Sandrone, G.; Malfatto, G.; Dell'Orto, S.; Piccaluga, E. Power spectral analysis of heart rate and arterial pressure variabilities as a marker of sympatho-vagal interaction in man and conscious dog. Circulation research 1986, 59, 178–193.

[41] Pomeranz, B; Macaulay, R.; Caudill, M.A.; Kutz, I.; Adam, D.; Gordon, D.; Kilborn, K.M.; Barger, A.C.; Shannon, D.C.; Cohen, R.J. Assessment of autonomic function in humans by heart rate spectral analysis. American Journal of Physiology-Heart and Circulatory Physiology 1985, 248, 151–153.

[42] Saul, J.P.; Rea, R.; Eckberg, D.L.; Berger, R.D.; Cohen, R.J. Heart rate and muscle sympathetic nerve variability during reflex changes of autonomic activity. American Journal of Physiology-Heart and Circulatory Physiology 1990, 258, H713–H721.

[43] Kovatchev, B.P.; Farhy, L.S.; Cao, H.; Griffin, M.P.; Lake, D.E.; Moorman, J.R.

Sample asymmetry analysis of heart rate characteristics with application to neonatal sepsis and systemic inflammatory response syndrome. Pediatric research 2003, 54, 892.

[44] Tulen, J; Boomsma, F.; MAN IN ′TVELD, A.J. Cardiovascular control and plasma catecholamines during rest and mental stress: effects of posture. Clinical Science 1999, 96, 567–576.

[45] Verlinde, D.; Beckers, F.; Ramaekers, D.; Aubert, A.E. Wavelet decomposition analysis of heart rate variability in aerobic athletes. Autonomic Neuroscience 2001, 90, 138–141.

[46] Shaffer, F.; Ginsberg, J.P. An overview of heart rate variability metrics and norms. Public Health Front. 2017, 258.

[47] Birse, R.M.; revised by Knowlden, P.E. Muirhead, Alexander (1848–1920), electrical engineer. Interactive Factory 2004.

[48] Rivera-Ruiz, M.; Cajavilca, C.; Varon, J. Einthoven's string galvanometer: the first electrocardiograph. Texas Heart Institute Journal 2008, 35, 174.

[49] Wikipedia, Taro Takemi. Available online: https://en.wikipedia.org/wiki/Taro_Takemi#cite ref-hsph 1-0 (accessed on 29 May 2022).

[50] Ogawa, M.; Kimura, Y.; Tamura, T.; Togawa, T. Fully automated ECG data acquisition in a bathtub. In Proceedings of the 18th Annual International Conference of the IEEE Engineering in Medicine and Biology Society, Amsterdam, Netherlands, 31 October-3 November 1996; pp. 55–56.

[51] Kawarada A.; Nambu M.; Tamura T.; Ishijima M.; Yamakoshi K.; Togawa T. Fully automated monitoring system of health status in daily life. In Proceedings of the 22nd Annual International Conference of the IEEE Engineering in Medicine and Biology Society, Chicago, IL, USA, 23-28 July 2000; pp. 531–533.

[52] Hellhammer, D.H.; Stone, A.A.; Hellhammer, J.; Broderick, J. Measuring stress. Encycl. Behav. Neurosci. 2010, 2, 186–191.

[53] McEwen, B.S. Stressed or stressed out: What is the difference? J. Psychiatry Neurosci. 2005, 30, 315.

[54] Goyal, A.; Singh, S.; Vir, D.; Pershad, D. Automation of stress recognition using subjective or objective measures. Psychol. Stud. 2016, 61, 348–364.

[55] Petrakova, L.; Boy, K.; Mittmann, L.; Möller, L.; Engler, H.; Schedlowski, M. Salivary alpha-amylase and noradrenaline responses to corticotropin-releasing hormone administration in humans. Biol. Psychol. 2017, 127, 34–39.

[56] Allen, A.P.; Kennedy, P.J.; Cryan, J.F.; Dinan, T.G.; Clarke, G. Biological and psychological markers of stress in humans: Focus on the Trier Social Stress Test. Neurosci. Biobehav. Rev. 2014, 38, 94–124.

[57] Alberdi, A.; Aztiria, A.; Basarab, A. Towards an automatic early stress recognition system for office environments based on multimodal measurements: A review. J. Biomed. Inform. 2016, 59, 49–75.

[58] Kaniusas, E. Fundamentals of biosignals. In Biomedical signals and sensors I. 2012, 1–26.

[59] Alonso, J.F.; Romero, S.; Ballester, M.R.; Antonijoan, R.M.; Mañanas, M.A. Stress assessment based on EEG univariate features and functional connectivity measures. Physiological measurement 2015, 36, 1351.

[60] Tokyo Gas Inc., Current situation of the manner of bathing in Japan. Available online: https://www.toshiken.com/report/docs/hot34-summary.pdf (accessed on 1 December 2021).

[61] Consumer Affairs Agency, Government of Japan, news release. Available online: https://www.caa.go.jp/policies/policy/consumer_safety/caution/caution_055/assets/caution_055_211208_0002.pdf (accessed on 1 May 2022).

[62] Li, T.; Chen, Y.; Chen, W. Daily Stress Monitoring Using Heart Rate Variability of Bathtub ECG Signals. 2018 40th Annual International Conference of the IEEE Engineering in Medicine and Biology Society (EMBC). IEEE, 2018.

[63] Mayya, S.; Jilla, V.; Tiwari, V.N.; Nayak M.M.; Narayanan, R. Continuous monitoring of stress on smartphone using heart rate variability. 2015 IEEE 15th International Conference on Bioinformatics and Bioengineering (BIBE). Belgrade, 2015, 1–5.

[64] Castaldo, R.; Melillo, P.; Bracale, U.; Caserta, M.; Triassi, M.; Pecchia, L. Acute mental stress assessment via short term HRV analysis in healthy adults: A systematic review with meta-analysis. Biomedical Signal Processing and Control 2015, 18, 370–377.

[65] Richman, J.S.; Moorman, J.R. Physiological time-series analysis using approximate entropy and sample entropy. Am J Physiol Heart Circ Physiol.

2000, 278, 2039–2049.

[66] Barahona, M.; Poon, C.S. Detection of nonlinear dynamics in short, noisy time series. Nature 1996, 381, 215–217.

[67] Motoi, K.; Kubota, S.; Ikarashi, A.; Nogawa, M.; Tanaka, S.; Nemoto, T.; Yamakoshi, K. Development of a fully automated network system for long-term health-care monitoring at home. Proceedings of the 29th Annual Conference of the IEEE Engineering in Medicine and Biology Society, pp. 1826-1829, 2007.

[68] Ogawa, M.; Tamura, T.; Togawa, T. Fully automated biosignal acquisition in daily routine through 1 month. Proceedings of the 20th Annual International Conference of the IEEE Engineering in Medicine and Biology Society, vol. 20, no. 4, pp. 1947-1950, 1998.

[69] Motoi, K.; Yamakoshi, Y.; Yamakoshi, T.; Sakai, H.; Tanaka, N.; Yamakoshi, K.I. Measurement of electrocardiograms in a bath through tap water utilizing capacitive coupling electrodes placed outside the bathtub wall. Biomedical engineering online 2017, 16, 1-13.

[70] Velayudhan, A.; Peter, S. Noise analysis and different denoising techniques of ECG signal-a survey. IOSR Journal of Electronics and Communication Engineering (IOSR-JECE) 2016, 40-44.

[71] Butt, M.; Razzaq, N.; Sadiq, I.; Salman, M.; Zaidi, T. Power Line Interference removal from ECG signal using SSRLS algorithm. Signal Processing and its Applications (CSPA) 2013 IEEE 9th International Colloquium on, pp. 95-98.

[72] Raphisak, P.; Schuckers, S.C.; Curry, A.J. An algorithm for EMG noise detection in large ECG data. Computers in Cardiology 2004, 31, 369-372.

[73] Thalkar, S.; Upasani, D. Various techniques for removal of power line interference from ECG signal, International Journal of Scientific & Engineering Research 2013, 4, 12-23.

[74] Friesen G.M.; Jannett, T.C. A comparison of the noise sensitivity of nine QRS detection algorithms. IEEE Trans. Biomed. Eng. 1990, 37, 85-98.

[75] Poungponsri, S.; Yu, X.H. Electrocardiogram (ECG) signal modeling and noise reduction using wavelet neural networks. Proc. IEEE Int. Conf. Autom. Logistics, pp. 394-398, Aug. 2009.

[76] Lim, Y.K.; Kim, K.K.; Park, K.S. The ECG measurement in the bathtub using the insulated electrodes. Proc. 26th Annu. Int. Conf. Engineering Medicine Biol. Soc. IEMBS, vol. 1, pp. 2383-2385, Sept. 2004.

[77] Wang, J.Y. A new method for evaluating ECG signal quality for multi-lead arrhythmia analysis. Comput. Cardiol. 2002, 29, 85-88.

[78] Orphanidou, C.; Bonnici, T.; Charlton, P.; Clifton, D.; Vallance, D.; Tarassenko, L. Signal-quality indices for the electrocardiogram and photoplethysmogram: derivation and applications to wireless monitoring. IEEE J Biomed Health Inform. 2015, 19, 832-838.

[79] Morgado, E.; Alonso-Atienza, F.; Santiago-Mozos, R.; Barquero-Pérez, Ó.; Silva, I.; Ramos, J.; Mark R. Quality estimation of the electrocardiogram using cross-correlation among leads. Biomed. Eng. Online 2015, 14, 59.

[80] Del Rio, B.A.S.; Lopetegi, T.; Romero, I. Assessment of different methods to estimate electrocardiogram signal quality. Proc. Comput. Cardiol. 2011, 609-612.

[81] Fletcher, G.F.; Ades, P.A.; Kligfield, P.; Arena, R.; Balady, G.J.; Bittner, V.A.; Coke, L.A.; Fleg, J.L.; Forman, D.E.; Gerber, T.C.; Gulati, M.; Madan, K.; Rhodes, J.; Thompson, P.D.; Williams, M.A. Exercise standards for testing and training: a scientific statement from the American Heart Association. Circulation 2013, 128, 873–934.

[82] Goldschlager, N.; SELZER, A.; Cohn, K. Treadmill stress tests as indicators of presence and severity of coronary artery disease. Ann. Intern. Med. 1976, 85, 277–286.

[83] Théroux, P.; Waters, D.D.; Halphen, C.; Debaisieux, J.C.; Mizgala, H.F. Prognostic value of exercise testing soon after myo-cardial infarction. New Eng. J. Med. 1979, 301, 341–345.

[84] Hochreiter C.; Borer J.S. Exercise testing in patients with aortic and mitral valve disease: current applications. Cardiovasc. Clin. 1983, 13, 291–300.

[85] Gentile, B.A.; Tighe, D.A. Exercise Stress ECG Test Protocols. In Pocket Guide to Stress Testing, 2nd ed.; Tighe, D.A., Gentile, B.A., Eds.; John Wiley & Sons, Ltd., 2019; pp. 53–66.

[86] Shah, B.N. On the 50th anniversary of the first description of a multistage exercise treadmill test: re-visiting the birth of the ‘Bruce protocol’. Heart 2013, 99, 1793–1794.

[87] Stuart, R.J.; Ellestad, M.H. National survey of exercise stress testing facilities. Chest 1980, 77, 94–7.

[88] Gibbons, R.J.; Balady, G.J.; Timothy Bricker, J.; Chaitman, B.R.; Fletcher, G.F.; Froelicher, V.F.; Mark, D.B.; McCallister, B.D.; Mooss, A.N.; O'Reilly, M.G.; Winters, W.L.; Antman, E.M.; Alpert, J.S.; Faxon, D.P.; Fuster, V.; Gregoratos, G.; Hiratzka, L.F.; Jacobs, A.K.; Russell, R.O.; Smith, S.C. ACC/AHA 2002 guideline update for exercise testing: summary article: a report of the American College of Cardiology/American Heart Association Task Force on Practice Guidelines (Committee to Update the 1997 Exercise Testing Guidelines). J. Am. Coll. Cardiol. 2002, 40, 1531–1540.

[89] Gibbons, R.J.; Balady, G.J.; Beasley, J.W.; Bricker, J.T.; Duvernoy, W.F.; Froelicher, V.F.; Mark, D.B.; Marwick, T.H.; McCallister, B.D.; Thompson, P.D.; Winters, W.L.; Yanowitz, F.G.; Ritchie, J.L.; Gibbons, R.J.; Cheitlin, M.D.; Eagle, K.A.; Gardner, T.J.; Garson, A.J.; Lewis, R.P.; O'Rourke, R.A.; Ryan, T.J. ACC/AHA Guidelines for Exercise Testing. A report of the American College of Cardiology/American Heart Association Task Force on Practice Guidelines (Committee on Exercise Testing). J. Am. Coll. Cardiol. 1997, 30, 260–311.

[90] Kwatra, S.C.; Jain, V.K. A new technique for monitoring heart signals-part I: instrumentation design. IEEE. Trans. Biomed. Eng. 1986, 1, 35–41.

[91] Tamura T.; Yoshimura T.; Nakajima K.; Miike H.; Togawa T. Unconstrained heart-rate monitoring during bathing. Biomed. Instrum. Technol. 1997, 31, 391–396.

[92] Mizukami, H.; Togawa, T.; Toyoshima, T.; Ishijima, M. Management of pacemaker patients by bathtub ECG. Iyo Kizai Kenkyujo hokoku. Reports of the Institute for Medical and Dental Engineering, Tokyo Medical and Dental University 1989, 23, 113–119.

[93] Xu J.; Chen, W. Impact of Water Temperature on Heart Rate Variability during Bathing. Life 2021, 11, 378.

[94] Xu, J.; Li, T.; Chen, Y.; Chen, W. Personal identification by convolutional neural network with ECG signal. In Proceedings of the 2018 International Conference on Information and Communication Technology Convergence, Jeju, Korea (South), 17-19 October 2018; pp. 559–563.

[95] Fletcher, G.F.; Balady, G.J.; Amsterdam, E.A.; Chaitman, B.; Eckel, R.; Fleg, J.; Froelicher, V.F.; Leon, A.S.; Piña, I.L.; Rodney, R.; Simons-Morton, D.A.; Williams, M.A.; Bazzarre, T. Exercise standards for testing and training: a statement for healthcare professionals from the American Heart Association. Circulation 2001, 104, 1694–1740.

[96] Gorman, A.J.; Proppe, D.W. Mechanisms producing tachycardia in conscious baboons during environmental heat stress. J. Appl. Physiol. 1984, 56, 441–446.

[97] Karthikeyan, P.; Murugappan, M.; Yaacob, S. Detection of human stress using short-term ECG and HRV signals. J. Mech. Med. Biol. 2013, 13, 1350038.

[98] Munla, N.; Khalil, M.; Shahin, A.; Mourad, A. Driver stress level detection using HRV analysis. In Proceedings of the 2015 international conference on advances in biomedical engineering, Beirut, Lebanon, 16-18 September 2015;

pp. 61–64.

[99] Ferdinando, H.; Seppänen, T.; Alasaarela, E. Comparing features from ECG pattern and HRV analysis for emotion recognition system. In Proceedings of the 2016 IEEE Conference on Computational Intelligence in Bioinformatics and Computational Biology, Chiang Mai, Thailand, 5-7 October 2016; pp. 1–6.

[100] Orphanidou, C.; Drobnjak, I. Quality assessment of ambulatory ECG using wavelet entropy of the HRV signal. IEEE J. Biomed. 2016, 21, 1216–1223.

[101] Zarei, A.; Asl, B.M. Automatic classification of apnea and normal subjects using new features extracted from HRV and ECG-derived respiration signals. Biomed. Signal Process. Control 2020, 59, 101927.

[102] Kataoka, Y.; Yoshida, F. The change of hemodynamics and heart rate variability on bathing by the gap of water temperature. Biomed. Pharmacother. 2005, 59, S92–S99.

[103] Edelhäuser, F.; Goebel, S.; Scheffer, C.; Cysarz, D. P02. 181. Heart rate variability and peripheral temperature during whole body immersion at different water temperatures. BMC Complement. Altern. Med. 2012, 12, 1.

[104] The Physics Factbook, Temperature of a Japanese Bath. Available online: https://hypertextbook.com/facts/2005/LouisWilliamTullo.shtml (accessed on 3 April 2022).

[105] Tun, H.M., Naing, Z.M., Moe, W.K., Latt, M.M. Analysis of heart rate variability based on quantitative approach. MOJ Proteomics Bioinform. 2018,

7, 131–141.

[106] Abdi, H.; Williams, L.J. Principal component analysis. Wiley interdisciplinary reviews: computational statistics 2010, 2, 433–459.

[107] Vidal, R.; MA, Y.; Sastry, S.S. Principal component analysis. In Generalized principal component analysis; Springer: New York, NY., USA, 2016; Volume 40, pp. 25–62.

[108] Tei, C.; Horikiri, Y.; Park, J.C.; Jeong, J.W.; Chang, K.S.; Toyama, Y.; Tanaka, N. Acute hemodynamic improvement by thermal vasodilation in congestive heart failure. Circulation 1995, 91, 2582–2590.

[109] Michalsen, A.; Lüdtke, R.; Bühring, M.; Spahn, G.; Langhorst, J.; Dobos, G.J. Thermal hydrotherapy improves quality of life and hemodynamic function in patients with chronic heart failure. Am. Heart J. 2013, 146, 728–733.

[110] Oyama, J.I.; Kudo, Y.; Maeda, T.; Node, K.; Makino, N. Hyperthermia by bathing in a hot spring improves cardiovascular functions and reduces the production of inflammatory cytokines in patients with chronic heart failure. Heart Vessels 2013, 28, 173–178.

[111] Kihara, T.; Biro, S.; Imamura, M.; Yoshifuku, S.; Takasaki, K.; Ikeda, Y.; Otuji Y.; Minagoe S.; Toyama, Y.; Tei, C. Repeated sauna treatment improves vascular endothelial and cardiac function in patients with chronic heart failure. J. Am. Coll. Cardiol. 2002, 39, 754–759.

[112] Blum, N.; Blum, A. Beneficial effects of sauna bathing for heart failure patients. Exp. Clin. Cardiol. 2007, 12, 29.

[113] Lee, J.; Park, B.J.; Tsunetsugu, Y.; Ohira, T.; Kagawa, T.; Miyazaki, Y. Effect of forest bathing on physiological and psychological responses in young Japanese male subjects. Public health 2011, 125, 93–100.